Science of the Total Environment 865 (2023) 161288

Contents lists available at ScienceDirect

Science of the Total Environment

journal homepage: www.elsevier.com/locate/scitotenv

The impact of local and climate change drivers on the formation, dynamics, and potential recurrence of a massive fish-killing microalgal bloom in Patagonian fjord

Patricio A. Díaz [a,b,*], Iván Pérez-Santos [a,c,d], Leila Basti [e,f], René Garreaud [g,h], Elias Pinilla [i,j], Facundo Barrera [a,h], Alfredo Tello [k], Camila Schwerter [a], Sara Arenas-Uribe [a], Camila Soto-Riquelme [i], Pilar Navarro [a], Manuel Díaz [l], Gonzalo Álvarez [m,n], Pamela M. Linford [a], Robinson Altamirano [a], Guido Mancilla-Gutiérrez [a], Camilo Rodríguez-Villegas [a,b], Rosa I. Figueroa [o]

[a] Centro i~mar, Universidad de Los Lagos, Casilla 557, Puerto Montt, Chile
[b] CeBiB, Universidad de Los Lagos, Casilla 557, Puerto Montt, Chile
[c] Center for Oceanographic Research COPAS Sur-Austral and COPAS COASTAL, Universidad de Concepción, Chile
[d] Centro de Investigaciones en Ecosistemas de la Patagonia (CIEP), Coyhaique, Chile
[e] Faculty of Marine Environment and Resources, Tokyo University of Marine Science and Technology, 108-8477 Tokyo, Japan
[f] College of Agriculture and Veterinary Science, Department of Integrative Agriculture, United Arab Emirates University, Al Ain, Abu Dhabi, United Arab Emirates
[g] Departamento de Geofísica, Universidad de Chile, Santiago 8370449, Región Metropolitana, Chile
[h] Centro de Ciencia del Clima y la Resiliencia (CR2), Universidad de Chile, Chile
[i] Instituto de Fomento Pesquero (IFOP), Putemún, Castro, Chile
[j] Department of Civil and Environmental Engineering, University of Maine, 5711 Boardman Hall, Orono, ME, USA
[k] Salmones Camanchaca S.A., Puerto Montt, Chile
[l] Instituto de Acuicultura & Programa de Investigación Pesquera, Universidad Austral de Chile, Los Pinos s/n, Puerto Montt, Chile
[m] Facultad de Ciencias del Mar, Departamento de Acuicultura, Universidad Católica del Norte, Coquimbo 1281, Chile
[n] Centro de Investigación y Desarrollo Tecnológico en Algas (CIDTA), Facultad de Ciencias del Mar, Larrondo 1281, Universidad Católica del Norte, Coquimbo, Chile
[o] Centro Oceanográfico de Vigo, Instituto Español de Oceanografía (IEO-CSIC), Vigo, Spain

HIGHLIGHTS

- Climate change drivers and local hydrodynamics fostered a massive bloom of *Heterosigma akashiwo* in a Patagonian fjord.
- Positive SAM phase promoted an increase in water temperature and upwelling.
- Salt-fingering events also transport nutrients to the photic layer.
- Hydrodynamic modelling shows that uplifts could promote the resuspension of microalgal benthic stages.

GRAPHICAL ABSTRACT

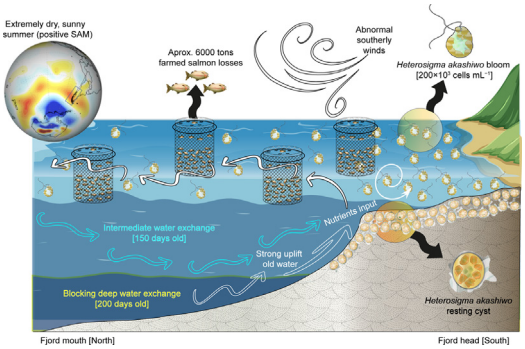

ARTICLE INFO

Editor: Daniel Wunderlin

Keywords:
Brown tide
Salmon mortality

ABSTRACT

Harmful algal blooms (HABs) in southern Chile are a serious threat to public health, tourism, artisanal fisheries, and aquaculture in this region. Ichthyotoxic HAB species have recently become a major annual threat to the Chilean salmon farming industry, due to their severe economic impacts. In early austral autumn 2021, an intense bloom of the raphidophyte *Heterosigma akashiwo* was detected in Comau Fjord, Chilean Patagonia, resulting in a high mortality of farmed salmon

* Corresponding author at: Centro i~mar & CeBiB, Universidad de Los Lagos, Casilla 557, Puerto Montt, Chile.
E-mail address: patricio.diaz@ulagos.cl (P.A. Díaz).

http://dx.doi.org/10.1016/j.scitotenv.2022.161288
Received 6 November 2022; Received in revised form 9 December 2022; Accepted 26 December 2022
Available online 30 December 2022

Southern Annular Mode (SAM)
Upwelling
Biogeochemistry
NW Chilean Patagonia
Climate anomalies

(nearly 6000 tons of biomass) within 15 days. *H. akashiwo* cells were first detected at the head of the fjord on March 16, 2021 (up to 478 cells mL^{-1}). On March 31, the cell density at the surface had reached a maximum of 2×10^5 cells mL^{-1}, with intense brown spots visible on the water surface. Strong and persistent high-pressure anomalies over the southern tip of South America, consistent with the positive phase of the Southern Annular Mode (SAM), resulted in extremely dry conditions, high solar radiation, and strong southerly winds. A coupling of these features with the high water retention times inside the fjord can explain the spatial-temporal dynamics of this bloom event. Other factors, such as the internal local physical uplift process (favored by the north-to-south orientation of the fjord), salt-fingering events, and the uplift of subantarctic deep-water renewal, likely resulted in the injection of nutrients into the euphotic layer, which in turn could have promoted cell growth and thus high microalgal cell densities, such as reached by the bloom.

1. Introduction

The massive proliferation of nuisance microalgae in marine, brackish water, or freshwater environments is responsible for substantial negative socio-economic impacts on fisheries, aquaculture, tourism, coastal and inland ecosystems, and public health. These proliferations are referred to as "harmful algal blooms," or HABs (Burkholder, 1998; Glibert et al., 2005; Landsberg, 2002; Van Dolah, 2000), and are generally classified into three types depending on the main effect of the bloom-forming microalgal species. The first type includes species that produce potent toxins that are bioamplified throughout the food web, reaching levels that are toxic to organisms belonging to higher trophic levels, including humans, by inducing various poisoning syndromes. The second type is formed by species that, through their high biomass alone, cause the mass mortality of aquatic organisms in addition to hampering human activities, via a reduction of dissolved oxygen, discoloration of the water, and the formation of dense foams. The third type of HAB species is not toxic to higher trophic levels but adversely affects invertebrates and fish, notably in aquaculture farms, although the physical and biochemical processes responsible for the restricted toxicity have yet to be fully elucidated (Hallegraeff, 2003).

While HABs are broadly regarded as naturally occurring phenomena, there has been a perceived trend of a global increase in their frequency and geographical distribution, in part due to the increasing implementation of monitoring programs but also in response to accelerated global change, including eutrophication, climate change, and the increase in aquaculture activities in marine and freshwater environments. Regional factors, such as an increase in thermohaline stratification, have also been implicated in the occurrence, frequency, bloom duration, and geographical distribution of microalgal harmful species (Glibert, 2020; Gobler et al., 2017; Hallegraeff et al., 2021; Wells et al., 2015).

In Chile, the negative effect of HABs have been mostly related to the toxic effects in humans induced following the consumption of contaminated shellfish (Clément et al., 2002; Fuentes et al., 2008; Mardones et al., 2020; Mardones et al., 2010; Molinet et al., 2003). The latter have mainly consisted of paralytic shellfish poisoning, due to the consumption of shellfish feeding on toxic *Alexandrium catenella* (Álvarez et al., 2019; Díaz et al., 2014; Díaz et al., 2022b), diarrheic shellfish poisoning, caused by toxic shellfish feeding on *Dinophysis* species (Díaz et al., 2022a), and amnesic shellfish poisoning, provoked by shellfish feeding on *Pseudo-nitszchia* spp. (Díaz et al., 2019; Suárez-Isla et al., 2002). However, massive fish-killer events caused by the ichthyotoxic microalgae *A. catenella*, *Karenia selliformis*, *Pseudochattonella verruculosa*, and *Heterosigma akashiwo* have also been recurrently reported in Chilean Patagonian fjords. Those events resulted in enormous losses of wild and farmed fish (Avaria et al., 1999; Díaz et al., 2019).

The first significant HAB fish-killing outbreak occurred in September 1988, subsequent to the expansion of the local aquaculture industry, which in the southernmost regions of the country (Los Lagos, Aysén and Magallanes) began in the 1980s (Díaz et al., 2019; Mardones et al., 2021). This HAB event of 1988 caused mass fish mortality, with the loss of >5000 tons of salmon, equivalent to almost 50 % of the total annual salmon production and an estimated economic loss of US$11 M (Avaria et al., 1999; Díaz et al., 2019). The culprit microalga was the raphidophyte *H. akashiwo*, a cosmopolitan species that forms blooms in coastal marine and brackish waters and whose lethality is mediated by the production of long-chain polyunsaturated fatty acids (Edvardsen and Imai, 2006; Kim et al., 2000; Twiner et al., 2001; Twiner et al., 2004) and/or other potentially toxic metabolites (Basti et al., 2021; Basti et al., 2016) as well as the induction of reactive oxygen species (ROS) in fish gills. Neurotoxic substances such as HaTx-i, HaTx-iia, HaTx-iib and HaTx-iii, which correspond to brevetoxin components PbTx-2, PbTx-9, PbTx-3 and oxidized PbTx-2, have also been identified in this species (Khan et al., 1997).

In 2016, a HAB caused by *P. verruculosa* led to the largest mass mortality of farmed fish on record, with the loss of almost 40,000 tons of fish from 45 Chilean salmon farms, corresponding to 18–20 % of the Chilean salmon production and a value of US$ 800 M (Clément et al., 2016; Mardones et al., 2021). The price of salmon subsequently increased by 25 % (FAO, 2016). Several climatic, hydrologic, and oceanographic factors were proposed to explain the bloom and the devastating damage it caused. These included the combined effects of radiative forcing, the El Niño Southern Oscillation (ENSO), and wind upwelling, which, together, strongly stratified the water column over several weeks, which in turn supported the proliferation of *P. verruculosa* (Garreaud, 2018; León-Muñoz et al., 2018; Mardones et al., 2021). However, species-specific differences in the environmental factors promoting the growth and toxicity of *P. verruculosa* and *H. akashiwo* have been determined, notably salinity and water temperature (Sandoval-Sanhueza et al., 2022).

In addition to the mass mortality of wild and farmed salmon, HABs can cause the death of deep-sea corals, including those in the fjords of Chile, via the decomposition of the enormous microalgal biomass, which sinks to the bottom and forms organic layers toxic to coral habitats (Försterra et al., 2014).

The most recent bloom of *H. akashiwo* occurred in early austral autumn 2021 and led to the loss of 6000 tons of farmed salmon, with an estimated economic loss of US$ 4.4 M, at 12 aquaculture facilities in the Comau Fjord (Los Lagos Region, Fig. 1) (Clément et al., 2021). The oceanographic, hydrologic, and climatological processes that contributed to this HAB event have yet to be investigated. In addition to its importance as a fish-farming site, Comau Fjord harbors complex, biodiverse ecosystems linked to its unique geological, climatic, and oceanic features. It is one of three highly pristine fjords in Chile, with its deep-sea coral ecosystems thriving in shallow to deep waters along an acidity gradient that extends well beyond the level of aragonite saturation included in the worst case scenario of climate change at the turn of the century (Fillinger and Richter, 2013; Jantsen et al., 2013; Maier et al., 2021).

As observed in other Patagonian coastal systems, Comau Fjord is a transitional system of estuarine-marine interfaces with a 10 m-surface layer of water that is poor in nitrates and phosphates but rich in organic matter and silicates, which arrive with the freshwater runoff from rivers. Surface and groundwater flows of the fjords are fed by an abundant rainfall and by glacier melting (Pantoja et al., 2011; Sánchez et al., 2011). Macronutrients flow landward through a high-salinity water mass, the modified subantarctic water (SAAW), thereby generating a two-layer, vertically sharp but horizontally gradual salinity gradient. Stratification of the water column from late winter to summer hinders primary production, while freshwater inputs in spring favor phytoplankton blooms mainly consisting of dinoflagellates (Meerhoff et al., 2019; Pérez-Santos et al., 2021; Sievers and Silva, 2008). However, the exceptional, complex interactions that characterize the hydrological dynamics of the fjords, along with the large-scale climatic conditions driven by SAM and ENSO give rise to HAB-favorable climatic-hydrological-

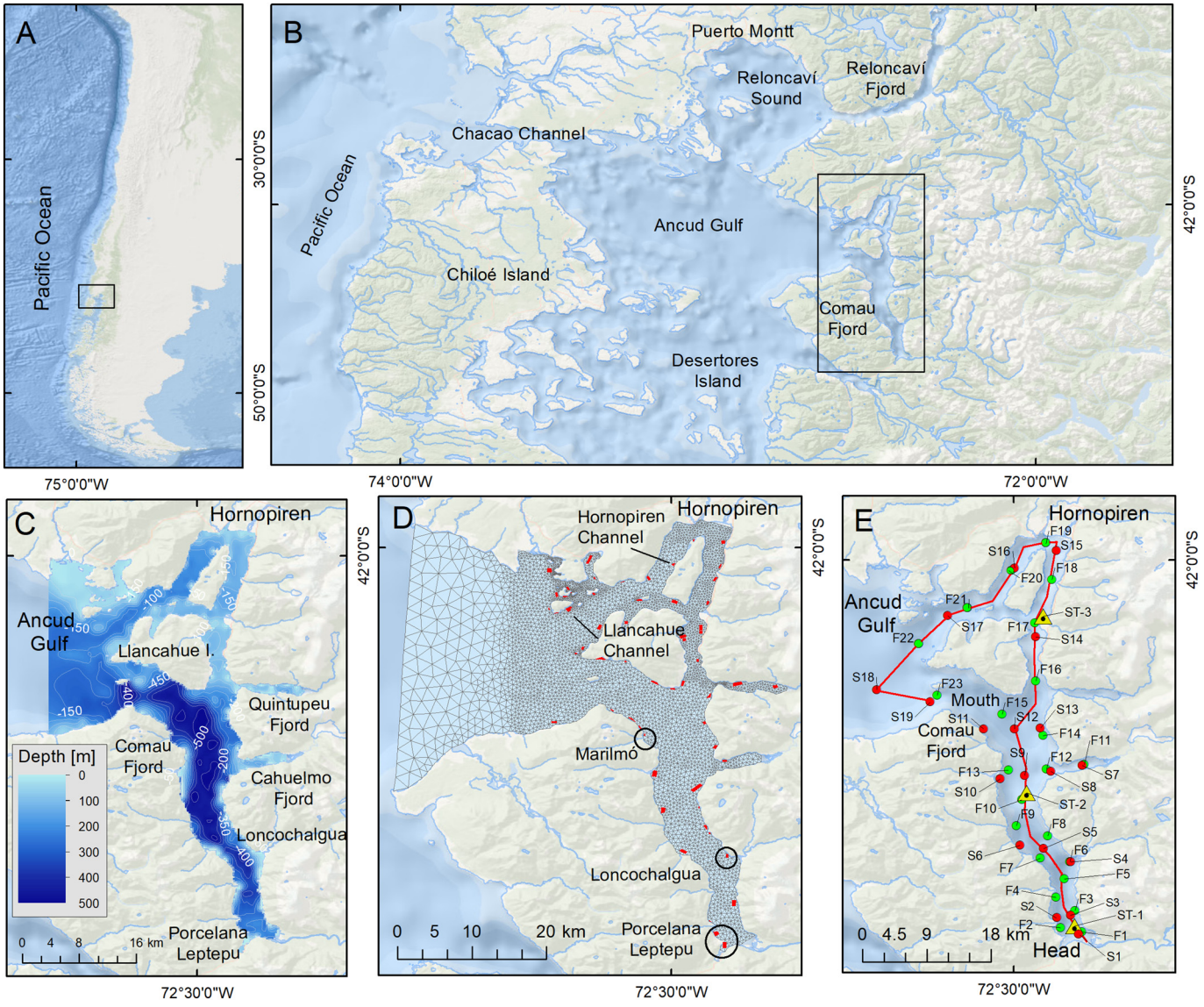

Fig. 1. Maps showing the study area. A) Chile; B) Northwestern Patagonia inland sea (the black box indicates Comau Fjord); C) Bathymetric map; D) Location of the sampling stations visited during summer (red circles) and fall (green circles) 2021; E) High-resolution model that includes Comau Fjord, Hornopirén, and the Llancahué channels in the north. Red rectangles show the locations of the salmon farms. (For interpretation of the references to colour in this figure legend, the reader is referred to the web version of this article.)

oceanographic conditions (Calvete and Sobarzo, 2011; Díaz et al., 2021; Díaz et al., 2016; Haury et al., 1978; Lucas and Largier, 2013; Roy et al., 2018). Given the risk of HABs to both the aquaculture industry and biodiversity, in this study we conducted a detailed investigation of the conditions that promote these events in Comau Fjord, with a focus on the conditions responsible for the recent large bloom of *H. akashiwo*. Our results enabled the formulation of a hypothesis explaining how the interplay between climatic, hydrological, and oceanographic dynamics led to the intense bloom of *H. akashiwo* observed in early austral autumn 2021 in Comau Fjord. We also assessed the impacts of the bloom on salmon aquaculture and local ecosystems.

2. Materials and methods

2.1. Study area

The southern coast of Chile, from 41° to 55° S, hosts one of the most extensive fjord and channel systems in the world (Fig. 1A–B). Large-volume freshwater inflows from rivers and the melting of glaciers results in a highly stratified system with a highly variable bathymetry and a highly dissected coastline. The region is also subject to heavy rainfall, especially over the windward side of the austral Andes, resulting in an annual average of 2700 mm and in some years up to 5000 mm (Pickard, 1971; Sauter, 2020). Rainfall occurs year-round but tends to decrease during austral summer, when more stable conditions lead to warmer air temperatures (Pérez-Santos et al., 2021).

Comau Fjord, among the northernmost Chilean fjords in Patagonia (42°15′ S), is part of this large fjord system. It is located adjacent to the Gulf of Ancud to the west and oriented from north to south, with a length of 34.3 km and a width ranging from 10 km at its mouth to 2 km near its head (Villalobos et al., 2021). The fjord has an average depth of ~412 m and a maximum depth of 497 m, with an abrupt change from 300 to 470 m at the mouth of the fjord that delimits a deep internal basin (Fig. 1C). The main freshwater sources are on the eastern side (Quintupeu and Cahuelmó Fjords) and at the headwaters (Vodudahue and Leptepu Rivers). The surface layer in winter is thicker and colder and has a lower salinity. During the relatively warmer summer, the salinity of the surface layer increases. Thus, at the surface layer the salinity fluctuates between 2 and 20 and the temperature between 7 and 20 °C. The water mass below the surface layer is of relatively constant salinity and temperature throughout the year (>32.5 and 11 °C, respectively; Häussermann and Försterra, 2009).

2.2. Climate data

Due to the rugged, isolated landscape of western Patagonia, there are only a few climatological stations with long-term records. However, the long-term, continuous records available from the Tepual weather station, near Puerto Montt City (41°26′S, 72°06 W), allow a detailed analysis of the interannual variability and trends in northern Patagonia, including Comau Fjord. For comparisons with the climate conditions during 2021, we obtained the CR2Met dataset (www.cr2.cl), which includes monthly gridded (0.05° × 0.05° lat-lon) data on the precipitation and temperature fields over Chile, from 1979 to 2022. CR2Met was built by the optimal interpolation of surface data from state-of-the-art European Centre reanalysis data (Álvarez-Garreton et al., 2018). The atmospheric circulation at a broader scale was analyzed using monthly means of sea level pressure (SLP), wind at selected pressure levels, and surface downward solar radiation, using data from 1970 to date, obtained from the National Centers for Environmental Prediction (NCEP)-National Center for Atmospheric Research (NCAR) Reanalysis and covering a 2.5° × 2.5° latitude-longitude grid (Kalnay et al., 1996). Monthly mean ENSO and Southern Annular Mode (SAM) indexes were obtained from the National Oceanographic Administration (NOAA) Physical Science Laboratory.

2.3. Field sampling

The field data used in this study were obtained from a monitoring program and from oceanographic cruises. In the former, phytoplankton cell counts and salmon mortality were determined daily at four sampling facilities. During the oceanographic cruises, hydrographic conditions, nutrients, chlorophyll *a*, and biogeochemical and other relevant parameters were recorded.

2.3.1. Monitoring program: phytoplankton and salmon mortality

Between March 15 and April 15, 2021, daily sampling was carried out as part of the Camanchaca Monitoring Program at four sampling stations located at salmon farms along Comau Fjord (Fig. 1D). Niskin bottles (5 L) were used to collect 100-mL water samples from four depths (sub-surface, 5, 10, 15 m) for quantitative analyses of phytoplankton. The samples were fixed with neutral Lugol's iodine solution (0.5–1 % final concentration) (Lovegrove, 1960), with aliquots then transferred to 10-mL chambers and then quantified using an inverted microscope after overnight sedimentation (Olympus CKX41), as described in Utermöhl (1958). The chamber was scanned at a magnification of ×200.

Daily salmon mortality rates at three farm facilities (Leptepu, Porcelana and Loncochalgua) between March 1 and May 1, 2021 were obtained from Camanchaca database.

2.3.2. Sampling during summer and autumn cruises

Two oceanographic cruises, were carried out in the Comau Fjord system in late summer (March 11–14) and mid-autumn (May 11–15) 2021, with the *R.V. Jurgen Winter* and *R.V. Centinella*, respectively. During both cruises, samples were taken along a 120-km transect (Fig. 1E): 19 stations during the late summer cruise (red full circles in Fig. 1E) and 23 stations during the mid-autumn cruise (green full circles in Fig. 1D). The transect began at the head of the Comau Fjord (stations S1 and S2), passed through the mouth of the fjord (station S11) before reaching the area near the town of Hornopirén (station S15), and then returned to the mouth of the fjord (station S19) (Fig. 1E).

Water samples for analyses of biogeochemical bulk parameters were collected at standard oceanographic depths (sub-surface, 5, 10, 25, 50, 75, 100, 150, 200, 300, 400 m) using 10-L Niskin bottles. In addition, sediment traps were moored at the head of the fjord (station 1), in the middle zone, in front of Cahuelmó Estuary (station 2), and at the mouth of the fjord (station 3) to evaluates fluxes and quality of organic matter in the water column during the mid-autumn cruise (see Fig. 1D for the locations).

Vertical profiles of temperature, salinity, and in vivo chlorophyll-*a* (Chl-a) fluorescence were obtained using an AML (model Metrec-XL) oceanographic CTD (conductivity, temperature, and depth) profiler (http://www.amloceanographic.com) equipped with a Turner Designs CYCLOPS-7 fluorometer (excitation 460 nm, emission, 620–715 nm), an optical sensor for dissolved oxygen (DO) determination, and other sensors to measure turbidity and pH. These parameters were measured at depths of 0–400 m at a sampling rate of 8 Hz. The temperature and salinity data from CTD were converted to conservative temperature (°C) and absolute salinity (S_A, in g kg^{-1}) according to the thermodynamic equation of seawater 2010 (IOC et al., 2010). The CTD data were processed using the software provided by the manufacturer and visualized using Ocean Data View software (Schlitzer, 2015).

2.3.3. Determination of inorganic nutrients and chlorophyll

Dissolved inorganic nutrients [NO_3^-, NO_2^-, PO_4^{3-}, and Si $(OH)_4$] were analyzed from 15-mL sea water samples, stored at −20 °C in HDPE bottles, using a Seal AA3 AutoAnalyzer according to the methodology described in Grasshoff et al. (1983) and the standard methods for seawater analysis (Kattner and Becker, 1991). The detection limit for the dissolved inorganic nutrients were: NO_3^- and NO_2^- (0.015 μM), PO_4^{3-} (0.010 μM), and Si $(OH)_4$ (0.030 μM). NH_4^+ analyses were omitted for logistical reasons, as the analysis of this labile molecule very soon after sample collection in remote areas in Southern Chile was not feasible. Chl-a, as a proxy of phytoplankton biomass, was fluorometrically determined following Strickland and Parson (1972) and Holm-Hansen et al. (1965), and expressed as μg L^{-1}.

2.3.4. Determination of biogeochemical bulk parameters after the HAB event

After the extreme HAB event in autumn 2021, intense sampling was conducted to evaluate its impact at molecular and biogeochemical levels. Suspended particulate matter (SPM), particulate organic carbon (POC), particulate organic nitrogen (PON), total nitrogen (TN), stables isotopes ($\delta^{13}C$ and $\delta^{15}N$), and Chl-a were measured in seawater (1 − 2 L) filtered through precombusted (450 °C, 4 h), 47-mm diameter, GF/F filters (0.7-μm pore size) at a pressure of 0.08 MPa, to avoid rupturing the plankton cells (Steinman et al., 2017). All filters were folded without rinsing, wrapped in aluminum foil, and immediately stored at −20 °C in an onboard freezer before they were brought back to the laboratory for further analysis.

SPM was determined by gravimetry based on the weight difference between the dried filter and the same filter before filtration (Grasshoff et al., 1999). Chl-a was fluorometrically determined as described above. Correction for phaeopigments was carried out by HCl (0.1 N) acidification of the samples.

Prior to the measurement of POC, TN, and their stable isotope ratios ($\delta^{13}C_{POC}$ and $\delta^{15}N_{TN}$) in the SPM samples, a filter was placed in a fumigation chamber with 5 mL of 10 N HCl for 24 h to remove inorganic carbon, following Verado et al. (1999) but with the modifications of Barrera et al. (2017). POC, TN, and their $\delta^{13}C_{POC}$ and $\delta^{15}N_{TN}$ values were determined at the Stable Isotope Facility of Pontifical University Catholic of Chile, using an elemental analyzer (EA Flash 2000 Thermo Finnigan) interfaced with a continuous-flow isotope ratio mass spectrometer (IRMS Delta V Advantage). The standard deviation (sd) was 0.2 ‰ for $\delta^{13}C$ and 0.3 ‰ for $\delta^{15}N$. Isotopic values are presented in standard δ-notation as per mL deviations relative to the conventional standards, i.e., VPDB (Vienna Pee Dee Belemnite) for carbon and atmospheric N_2 for nitrogen, as shown in Eqs. (I) and (II):

$$R = \frac{^{12}C}{^{13}C} \text{ ó } \frac{^{14}N}{^{15}N} \quad \text{(I)}$$

$$\delta X(\%O) = \left[\left(\frac{R_{sample}}{R_{standard}}\right) - 1\right] * 100 \quad \text{(II)}$$

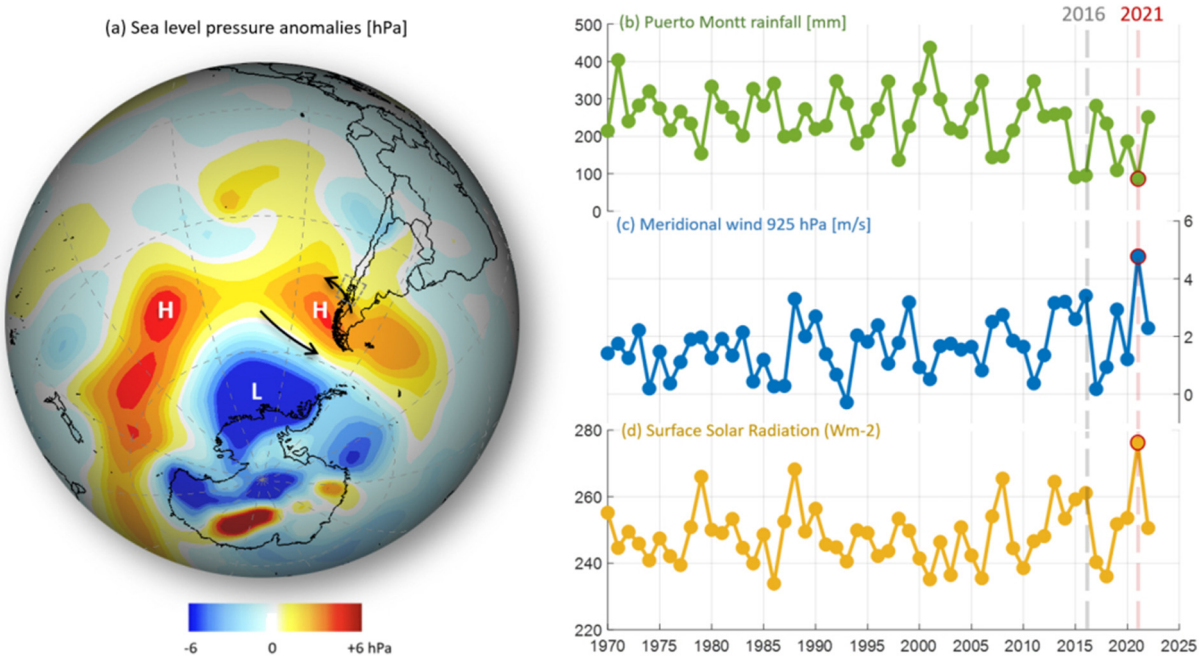

Fig. 2. Climate conditions. (a) Sea level pressure (SLP) anomalies during austral summer (Jan, Feb, Mar) 2021, calculated as departures from the long-term-mean (1980–2010). The letter H (L) indicates prominent centers of positive (negative anomalies). The curved arrows indicate the low-level wind anomalies induced by the positive SLP anomaly off the coast of southern Patagonia. (b) Austral-summer-accumulated precipitation at Puerto Montt (El Tepual). (c) Summer mean southerly winds at 925 hPa (about 800 m above sea level) over a grid box centered over Comau. (d) Summer mean solar radiation at the surface over a grid box centered over Comau. Data for (a), (c) and (d) from the NCEP-NCAR Reanalysis. Data from (b) from the Dirección Meteorologica de Chile.

where $R = {}^{13}C/{}^{12}C$ or ${}^{15}N/{}^{14}N$, (Peterson and Fry, 1987), R_{sample} and $R_{standard}$ are the heavy (${}^{13}C$ or ${}^{15}N$) to light (${}^{12}C$ or ${}^{14}N$) isotope ratios of the sample and standard, respectively, and X = ${}^{13}C$ or ${}^{15}N$ (e.g. Selvaraj et al., 2015).

The relative importance of allochthonous and autochthonous organic matter was calculated using two source end-member mixing models (Bianchi, 2007; González et al., 2019). Since the sum of the autochthonous marine (f_M) and allochthonous terrestrial (f_T) fractions of organic carbon and nitrogen, respectively, is 1, then:

$$\%POC_{terr} = \frac{\left(\delta^{13}C_s - \delta^{13}C_m\right)}{\left(\delta^{13}C_t - \delta^{13}C_m\right)} \quad \text{(III)}$$

Fig. 3. Red tide caused by *Heterosigma akashiwo*. The photograph was taken close to the head of Comau Fjord on April 4, 2021. (For interpretation of the references to colour in this figure legend, the reader is referred to the web version of this article.)

where $\delta^{13}C_s$ is the isotopic composition of a sample, $\delta^{13}C_m$ is the marine end-member from more oceanic stations (−17 ‰), and $\delta^{13}C_t$ terrestrial is the riverine/lake end-member value for POC (−30 ‰) as proposed for this area by González et al. (2019).

2.4. Hydrodynamics model and water renewal

The physical-oceanographic characteristics of Comau Fjord's circulation and transport were examined using the hydrodynamic model MIKE 3 FM (DHI, 2019), which solves the continuity, momentum, temperature, and salinity transport equations. The mathematical systems, parameterizations, and other specific characteristics of the MIKE 3 FM are reported in DHI (2019).

Comau Fjord, as well as the northern region, Hornopirén, and the Llancahué channels are included in the high-resolution model domain (Fig. 1D). SHOA nautical chart soundings were used to establish the bathymetry, with the natural neighbor approach then applied to create a digital elevation model (Sibson, 1981). Triangular elements of various sizes were used to discretize the resulting domain (Fig. 1D), with a higher resolution (average element size of 300 m) obtained for the coastline and shallow areas than for Comau Fjord's deep zone (500 m).

The modelling period spanned 3 years (2016–2018), with the boundary conditions of temperature, salinity, currents, and sea level provided using a regional hydrodynamic model (Pinilla et al., 2020) assessed and applied in other investigations (Díaz et al., 2021; Mardones et al., 2021). In the model, wind stress and heat fluxes are introduced over the sea surface based on the spatially and temporally variable fields of the WRF-IFOP atmospheric model. The performance of the WRF model was evaluated in Pinilla et al. (2020).

The freshwater sources originated from the hydrological model FLOW-IFOP, which employs the temperature and precipitation series from the 5 × 5 km spatially resolved CR2Met gridded product (http://www.cr2.cl/datos-productos-grillados/). The data are used to simulate runoff and to compute daily discharge series. For the years 2016–2018, the average annual freshwater discharge at Comau Fjord was 283 $m^3 s^{-1}$, which is equivalent to one-third of the freshwater entering the Reloncaví Fjord system, the area's largest freshwater basin (Fig. 1B). The CHONOS website (chonos.ifop.cl/flow/) provides information on the performance of the FLOW-IFOP model at the gauged river stations of the Chilean Water Authority.

The Regional Hydrodynamic Model, WRF Atmosphere Model, and FLOW Hydrological Model were constructed by the Instituto de Fomento Pesquero (www.ifop.cl). A complete description of all three can be found in Pinilla et al. (2020). The models are publicly accessible on the CHONOS website (chonos.ifop.cl) (Reche et al., 2021).

The water age approach (Bolin and Rodhe, 1973; Delhez et al., 1999; Monsen et al., 2002), which measures how long a water parcel has resided within a body of water (in this study, the fjord) after its entry, was used to calculate water renewal. This method has been used in other Patagonian fjords (Pinilla et al., 2020). Areas with an older water age are those in which the water parcel has resided in the fjord for a longer time. In the current work, water age was integrated into the Ecolab module of MIKE 3 FM linked to the hydrodynamic model and used to evaluate the spatial and temporal variability of water renewal within Comau Fjord.

The CTD records obtained in Comau Fjord during December 2020 (9 profiles), March 2021 (9 profiles), May 2021 (13 profiles), and June 2021 (9 profiles) were compared with the hydrodynamic model (2016–2018) (Fig. 1D). The goal was to replicate the water renewal process of deep and intermediate waters, which is modulated by the influx of salty water from the ocean. Salinity served as the tracer, and the depth of the 33 isohaline over 1 year as the reference. Note that the model and the observations are from different years. Fig. S1 of the Supplemental Material shows the results.

3. Results

3.1. Climate conditions

The SAM was in its positive phase during the austral summer (Jan–March) 2021, in connection with a circumpolar ring of high-pressure anomalies at mid-latitudes (Fig. 2A). SLP positive anomalies were particularly marked along a center straddling the southern tip of the continent and reached a maximum in February 2021. The rainfall in Puerto Montt during the 2021's austral summer reached a record low (Fig. 2B), with values slightly lower than those recorded in 2015, 2016, and 2019. The extremely dry conditions in late summer and early fall of 2021, with moisture deficits >60 %, encompassed most of southern Chile and western Patagonia (except south of 50°S) but resolved later, in April and May. The reduced number of storms crossing northern Patagonia was consistent with the significantly higher amounts of solar radiation that reached the surface in this area (Fig. 2D). The lack of precipitation over land led to substantial, almost immediate reductions in river discharge (e.g. Aguayo et al., 2019). For instance, the summer mean discharge in 2021 at the Carrera Basilio gauging station, in the Puelo River (just north of Comau Fjord), was ~60 % of the long-term mean. During the austral summer of 2021, air temperatures in northern Patagonia were above normal, including an extreme heat wave over inland sectors in early February.

The persistent positive pressure anomalies off western Patagonia also induced strong winds blowing from south to north (Fig. 2A) over Comau Fjord. Notably, at 925 hPa (about 800 m above sea level) the summer mean southerly winds in 2021 were larger than at any time during the 40-year record (Fig. 2C).

3.2. H. akashiwo bloom dynamics

A particularly intense bloom of *H. akashiwo* occurred at the end of summer and early fall of 2021 in Comau Fjord, NW Patagonia, creating dark brown patches close to the head of the fjord (Fig. 3). The increases in *H. akashiwo* densities (measured during the daily monitoring program) at four sampling stations in Comau Fjord from March 22 to April 8 showed a broad spatiotemporal variability (Fig. 4). On March 22rd, *H. akashiwo* cells were not detected (Fig. 4A) but on March 23rd *H. akashiwo* densities at the Leptepu salmon farm, located at the head of the fjord, were >20 cells mL^{-1} (Fig. 4B). Four days later (March 27), higher densities (>2 × 10^3 cells mL^{-1}) were recorded at two salmon farms (Leptepu and Porcelana) located at the head of the fjord (Fig. 4F). In both cases, microalgal cell numbers increased exponentially (Fig. 4S, T). The highest *H. akashiwo* cell density occurred at the Porcelana salmon farm on March 31st, with values >2 × 10^5 cells mL^{-1} measured at the sub-surface (Fig. 4J, T). During this period, the phytoplankton community at the sampled depths was completely dominated by *H. akashiwo* (>99.6 %). Extremely high densities (>2 × 10^4 cells mL^{-1}) were maintained at the head of the fjord until April 5th (Fig. 4K, L). Cell densities were significantly lower (1 × 10^3 cells mL^{-1}) at Marilmo salmon farm, located at the mouth of the fjord (Fig. 4C).

3.3. Salmon mortality temporal evolution

The intense bloom of *H. akashiwo* severely impacted the salmon farms located close to the head of Comau Fjord (Fig. 5A–C). A high daily salmon mortality (>40 tons) was first detected at the head of the fjord (Leptepu farm) on March 28 (Fig. 5A), where cell densities of *H. akashiwo* were ~ 17.4 × 10^3 cells mL^{-1} (Fig. 4G). Daily salmon mortality peaked between March 28 and 31, with the loss of >80 tons of fish per day. This large-scale fish mortality, which accounted for >70 % (1366 tons) of the total mortality recorded between March 28 and April 10, coincided with the highest densities of *H. akashiwo* during the bloom (1 × 10^5 to 2 × 10^5 cells mL^{-1}). At Leptepu farm, the total loss of salmon during the bloom event was 284 tons, corresponding to 57.2 % of its total production (Fig. 5A). At Porcelana and at Loncochalgua farms, located towards the

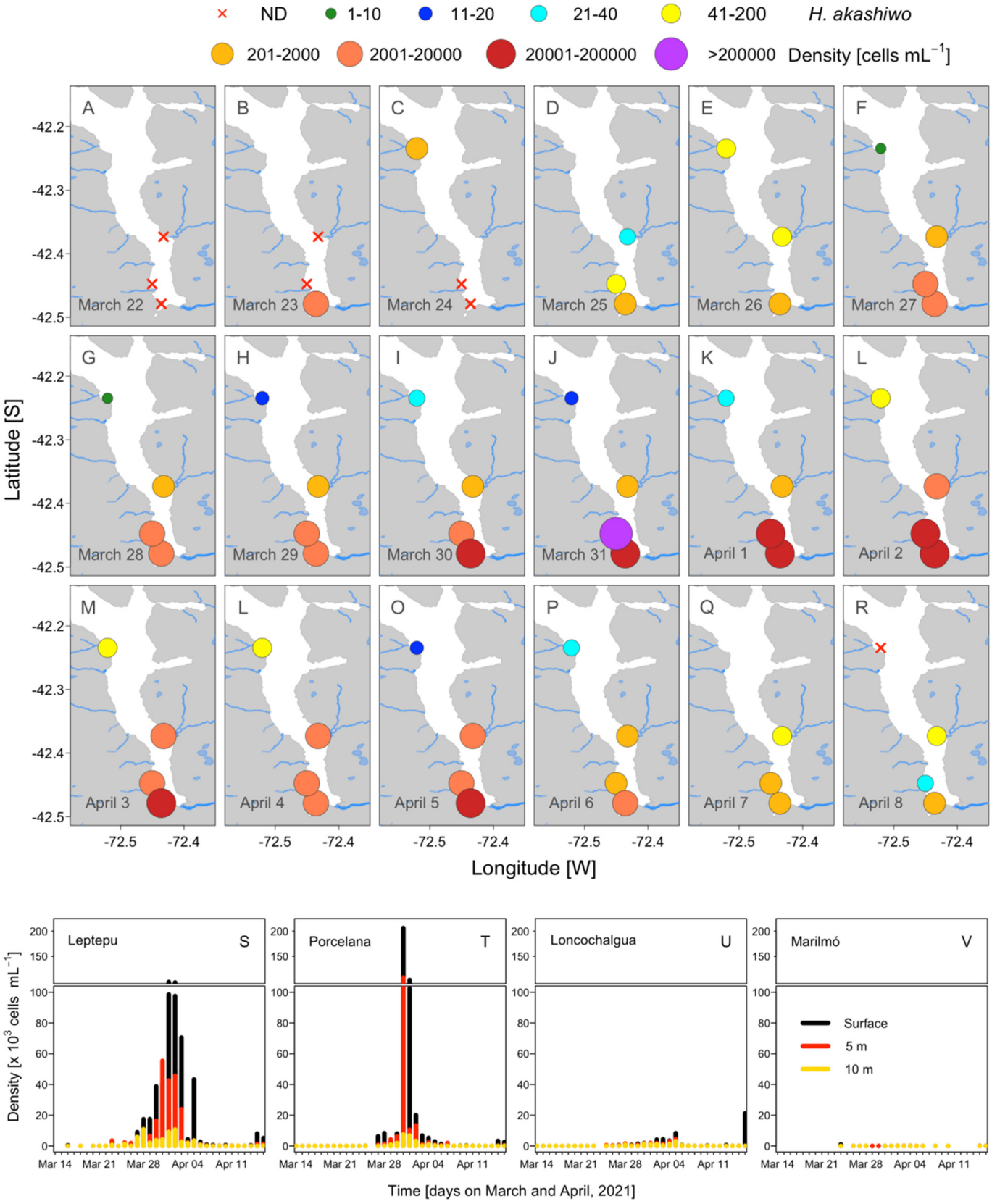

Fig. 4. Daily variation of *Heterosigma akashiwo* cell densities (data from the Camanchaca Monitoring Program) at four salmon farms in Comau Fjord. A–R) Surface distribution from March 22 to April 8, 2021; S–V) surface and subsurface distribution (0, 5, 10 m) from March 14 to April 16, 2021.

head of the fjord, the impact of the *H. akashiwo* bloom on salmon mortality was even greater, with total losses of 671 tons (maximum daily loss of 158 tons) and 903 tons (maximum daily loss of 183 tons), corresponding to 65.4 % and 100 % of the total production of these farms, respectively (Fig. 5B). At both salmon farms, at least two waves of mortality were recorded and were associated with increases in the cell density of

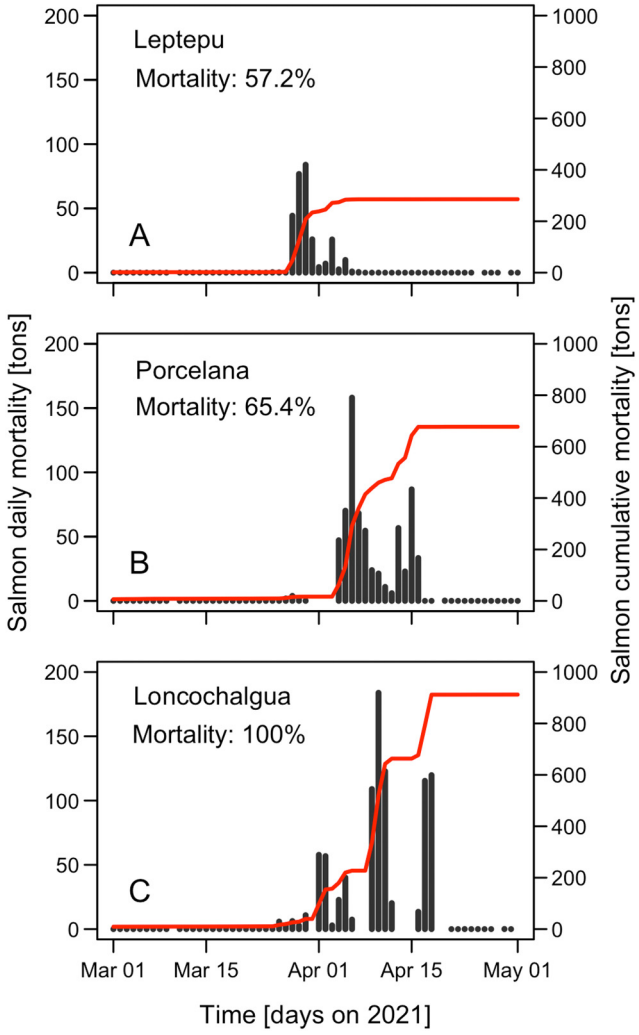

Fig. 5. Daily evolution of Atlantic salmon (*Salmo salar*) mortality from March 1 to May 1, 2021 at three salmon farms located in Comau Fjord.

H. akashiwo (Fig. 5B,C). The second wave occurred at Loncochalgua farm between April 15 and 16, when daily losses reached 115 tons and microalgal cell densities were >2 × 10^4 cells mL^{-1}.

3.4. Hydrographic conditions

The highest conservative surface temperature in 2021 was 18 °C, measured at the photic layer (0–20 m depth) at the end of summer (March) (Fig. 6A), concomitant with the detection of estuarine freshwater and oxygen-oversaturated water in the same layer and period (Fig. 6B, C). Significant reductions in the temperature in this 0- to 20-m upper layer occurred during the fall (May) mainly due to diminished solar radiation and ice melting (Fig. 6D–F). In addition, the surface decrease in DO reflected an increase in the layer of low DO (DO >60 % saturation), located between 20 and 100 m depth (Fig. 6F).

In the bottom layer (30 m above the bottom), seasonal features included a nucleus of low water temperature (minimum of 10.7 °C) at depths of 150–350 m depth during summer; but its area decreased in fall (Fig. 6A, D). An expansion of the SAAW occurred as well (Fig. 6E) and coincided with an increase in the extent of the low DO layer (Fig. 6F).

3.5. Inorganic nutrients

Mean nitrate concentration in March was 9.07 ± 7.93 μmoles L^{-1}, with a depletion at the surface and an increase at the bottom layers (Fig. 7A). A significant bottom-up increase towards the head of the fjord was also determined. The average nitrate concentration was higher in May than that at the end of summer, with a mean but highly variable value of 18.69 μmoles L^{-1} (sd = 8.55 μmoles L^{-1}). This was approximately 50 % higher than the value at depths of 5 and 10 m (Fig. 7A, D), where nitrate depletion at the surface resulted in a nitracline of 10 μmoles L^{-1} (Fig. 7D). In the middle layer (20–110 m), the nitrate concentration increased, reaching an average of 24.60 μmoles L^{-1}, and a maximum (29 μmoles L^{-1}) near the head of the fjord. From 110 m downwards, there was a progressive decrease in the nitrate concentration, with a nitracline of 20 μmoles L^{-1} detected between 20 and 200 m.

The average phosphate concentration in late austral summer was 1.41 ± 0.86 μmoles L^{-1} (Fig. 7B). The surface (0–20 m) concentration of <1.75 μmoles L^{-1} was consistent with a natural bottom-up decrease in the phosphate concentration and maximum value of 2.75 μmoles L^{-1} at the head of the fjord. A weak increase, similar to that determined for nitrates, was measured in the surface waters, at a depth of ~7 m, at the head of the fjord. In mid-autumn, the average phosphate concentration was 1.79 ± 0.63 μmoles L^{-1} (Fig. 7E). The vertical distribution showed that the lowest concentration (<1 μmoles L^{-1}) was in the upper 5 m, with decreasing concentrations at the head and mouth of the fjord. Similarly, the silicates concentration in the surface layer was low, with an average of 11.03 ± 7.0 μmoles L^{-1} in March, and a maximum of 28.24 μmoles L^{-1} at the bottom in the intermediate zone of the fjord (Fig. 7C). Also in March, a homogeneous deep layer of silicates was detected at all sampling sites. In May, the average silicates concentration was 17.10 ± 8.24 μmoles L^{-1} (Fig. 7F), with the highest concentrations occurring at depths between 50 and 300 m and an absolute maximum of 35.87 μmoles L^{-1} close to Hornopirén (station F19).

3.6. Biogeochemical bulks parameters after the HAB event

The average SPM concentration in Comau Fjord in May was 3.27 ± 1.52 mg L^{-1} (Fig. 8A). The highest concentration (>10 mg L^{-1}) occurred at the surface layer near the mouth of the fjord. From the surface to the bottom layer (~200 m), there was a significant decrease. High concentrations of Chl-a (>15 μg L^{-1}) were measured at sites where the SPM concentration was highest (Fig. 8B). Similar results were observed for POC and PON, with maximum values occurring at the surface layer (POC = 50–100 μmol L^{-1} and PON = 5–10 μmol L^{-1}, respectively). POC-PON values were highest in the surface waters inside Comau Fjord and decreased with depth, whereas they were lowest (<1 μmol L^{-1}) at the station area near Hornopirén and in the Gulf of Ancud (Fig. 8C, D).

The C:N ratio is often used as a proxy to trace the source and fate of organic matter in the fjord. Relatively high ratios were determined throughout the water column, with a mean of 12.59 ± 5.8. The C:N ratio was lowest (~8) at the surface layer and highest at the middle layer, from below 100 m depth to the bottom, and at the fjord head zone, where a nucleus with a high C:N (18–28) was detected (Fig. 9A). Organic carbon (C.org) correlated significantly with TN; the correlation was fitted to a linear regression (C.org = 7.66 NPT + 4.78; R^2 = 0.94).

The carbon isotope signal was low in the same areas where the C:N ratio was high ($\delta^{13}C_{POC}$ - 43.35 %) whereas enrichment was evident in waters from the head to the mouth and close to the surface layer (Fig. 9B). An isotopic enrichment in nitrogen characterized nearly the entire water column, with mean values of δ^{15}TN 8.84 ± 2.31 ‰ (Fig. 9C). A significant, negative correlation was determined for the relationship between $\delta^{13}C_{POC}$ and the C:N ratio, with a depletion of the isotopic signal as the C:N ratio increased (Fig. 9D). This relationship was highly significant (R^2 = 0.96) at the surface layer (<20 m) and significant towards the bottom (R^2 = 0.72), consistent with an isotopic fractionation of >9 ‰. The biogeochemical dynamics of organic matter degradation in Comau Fjord could be inferred from the relationship between DO and pH (Fig. 9E, F). The pH decreased as the C:N ratio increased. Regarding the relation between POC-PON and DO, there was a weak correlation between POC and DO (R^2_{POC} = 0.48) and a significantly

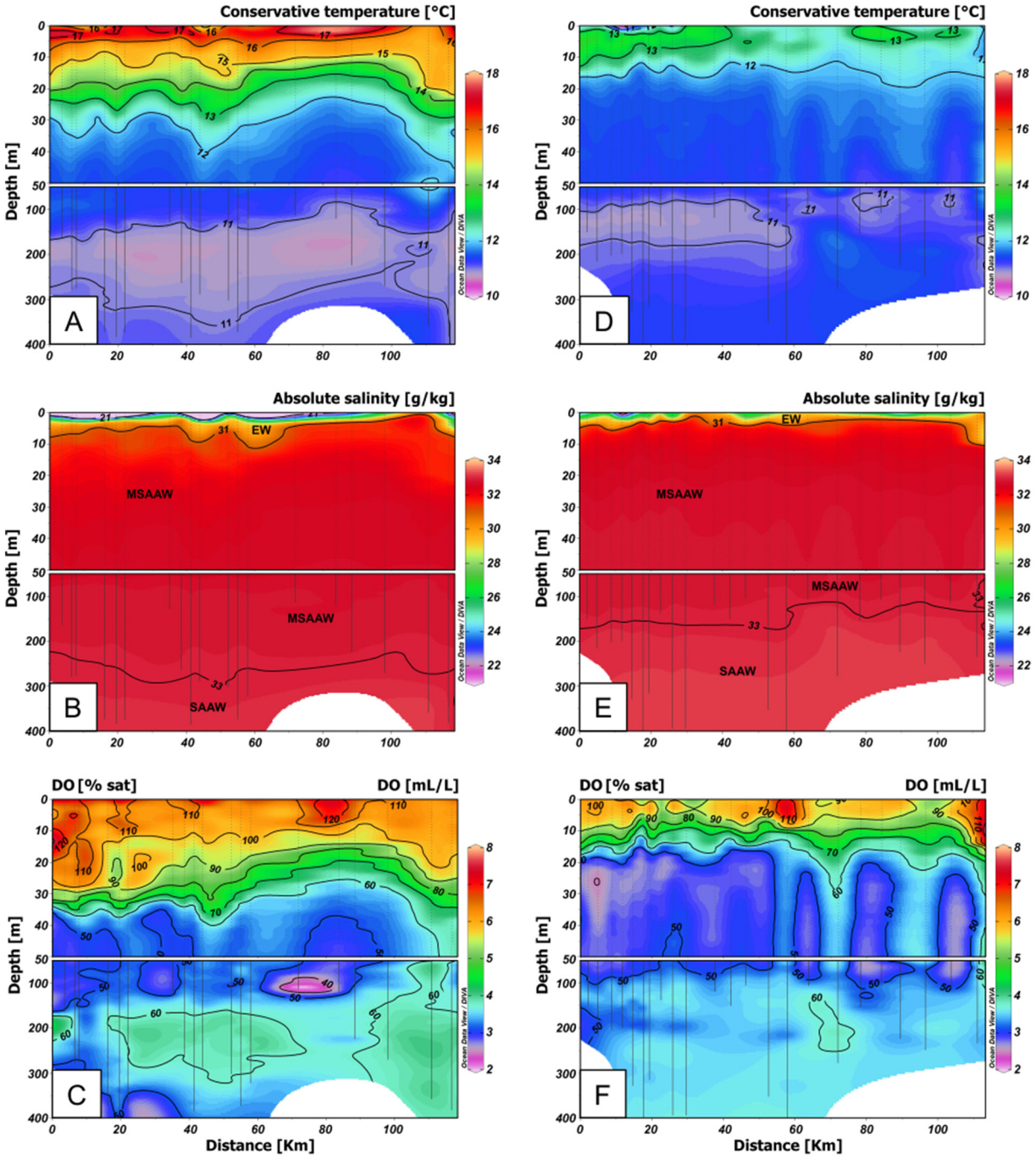

Fig. 6. Vertical distribution of conservative temperature (°C), absolute salinity (g kg^{-1}), and dissolved oxygen (mL L^{-1}) from 0 to 400 m along a transect in Comau Fjord during late summer (March; left panels) and middle fall (May; right panels) 2021.

strong correlation between PON and DO (R^2_{PON} = 0.65); both could be fitted to an exponential equation.

3.7. Fluxes and quality of organic matter in the water column

Estimations of the vertical fluxes of organic matter (C and N) are shown in Fig. 10. A high sedimentation rate of both C and N was determined at the head and mouth of the fjord (Fig. 10A, B). The analysis of $\delta^{13}C_{POC}$ vs. C:N showed the enrichment of carbon at the middle zone of the fjord (with a ratio close to 6), while the organic material content at the head of the fjord was smaller, with an increase of the C:N ratio (Fig. 10C). The relationship between the C and N isotopes showed that both the C and the N content were significantly depleted at the head of the fjord compared to the middle zone and mouth (2 ‰ and 1–1.5 ‰, respectively) (Fig. 10D).

3.8. Circulation patterns and water renewal

We performed a hydrodynamic simulation for the years 2016–2018 to obtain a complete picture of the complex ocean circulation within the fjord. The hydrodynamic model showed a mean surface circulation pattern (upper 10 m) in late summer (February and March) (Fig. 11A, B) that was characterized by weak currents (<2 cm s^{-1}) and an eddy-like pattern towards the mouth and head of the fjord. However, the water at the head was roughly twice as old as the water at the mouth, and its age increased

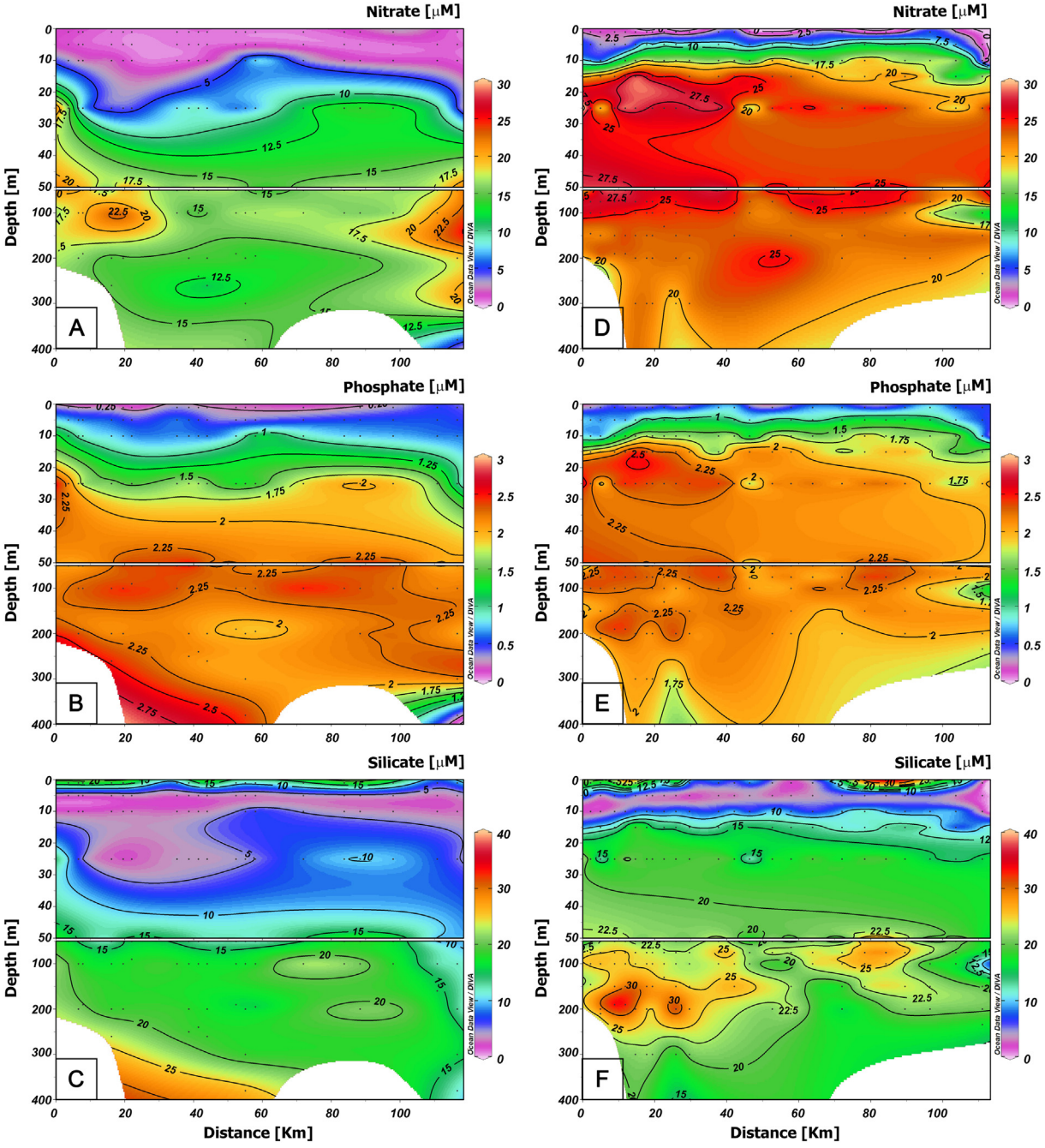

Fig. 7. Vertical distribution of nitrate (μM), phosphate (μM), and silicate (μM), from 0 to 400 m along a transect in Comau Fjord during late summer (March; left panels) and middle fall (May; right panels) 2021.

from 150 days in February to 200 days in April (Fig. 11G–I). There was also a noticeable change in the circulation pattern during April, with a stronger outflow from the fjord than in summer (Fig. 11C), especially towards the mouth (~10 cm s^{-1}). This outflow disrupted the summer's eddy-like pattern at the surface and caused a notable increase in water age in the fjord, with a maximum value of close to 200 days at the head (Fig. 11I).

The circulation was maintained with the fjord outflow from fall (May, June) (Fig. 11D,E) to winter (July) (Fig. 11F), with the highest values occurring in the latter season. The water age declined from May to July (~100 days) The yearly cycle of surface water age at the head of the fjord (Fig. 11M) consisted of an increase that began near the end of summer (100–150 days), peaked in the fall (~200 days), and then gradually declined in winter (~50 days).

An examination of the water exchange mechanisms in the fjord's deep and intermediate layers revealed intensive water exchange between the inner and outer fjord in winter, such that the water age is lower (50 days) than at other times of the year (Fig. 12A).

In the spring, a blockade at the fjord's mouth reduced water exchange such that the water age increased by ~100 days (Fig. 12B). Although the deep water at the mouth of the fjord was stagnant during summer, the rise of older water was observed at the head, caused by internal waves in the intermediate layer produced by modest water exchange (190 days) (Fig. 12C).

Oceanic water was transported into the fjord via the intermediate layer (50–300 m) early in the fall (Fig. 12D), such that this layer was renewed. This occurred along with a strong uplift of the older waters (~200 days)

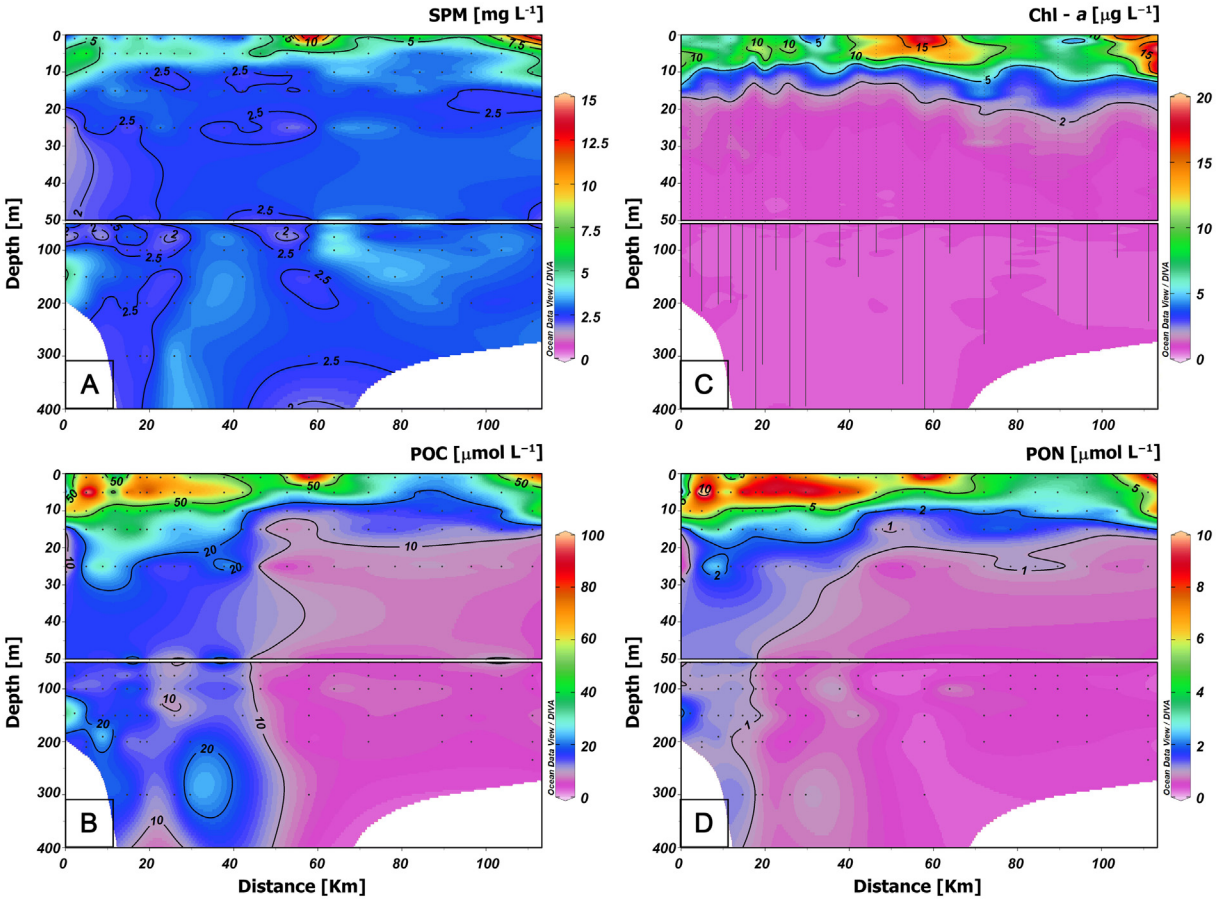

Fig. 8. Distribution of biogeochemical parameters along Comau Fjord after the HAB event. A) Suspended particulate matter (SPM, mg L^{-1}); B) chlorophyll-*a* (Chl-a, μg L^{-1}); C) particulate organic carbon (POC, μmol L^{-1}); D) particulate total nitrogen (PTN, μmol L^{-1}).

towards the head, such that they reach the surface layer, whereas water in the deep layer (300–470 m) was stagnant, with an age of ~230 days. Finally, in late fall, deep-water renewal replaced stagnant water in the deep layer of the fjord via the surface and intermediate layers (Fig. 12E).

4. Discussion

The frequency of HAB events in Chile is steadily increasing and spreading to new areas of Patagonian fjords and channels. While much of this increase, like HAB events elsewhere in the world, is related to climate change (Griffith and Gobler, 2020), the contributions of local and near-term environmental factors must be considered to predict individual events (Townhill et al., 2018). The intense HAB of the microalgae *H. akashiwo* in Comau Fjord in March 2021 caused extremely high losses of locally farmed salmon. In the following, we present and discuss our hypothesis on how the interaction between climatic, hydrological, and oceanographic drivers can lead to the development of the massive *H. akashiwo* bloom in Comau Fjord, such as occurred in March 2021. These drivers are diverse and include large-scale climate regulation from Antarctica to the Tropical Pacific Ocean, the physical and chemical conditions of the water column, and the water circulation regime across several water depth layers. Support for our hypothesis was obtained by analyzing the biogeochemical parameters of the water column during the bloom event that are relevant to microalgal growth.

4.1. Regional and local climate regulation

The extremely dry summer over western Patagonia in 2021 was consistent with a trend, observed since early 1980s (Boisier et al., 2018; Garreaud et al., 2021) (Fig. 2B) that has been attributed to the persistence of the SAM in its positive phase during the austral summer (e.g. Fogt and Marshall, 2020). This positive SAM phase is characterized by strong westerly winds around the (upper and lower) Antarctic coupled with a decrease in pressure over the Antarctic and an increase in surface pressure at midlatitudes. These pressure anomalies caused an abnormal expansion of the high-pressure cell over the subtropical SE Pacific towards southern Chile, resulting in a reduction of the westerly winds impinging on the austral Andes and a poleward shift of the storm track away from northern Patagonia (Garreaud, 2007). These features pushed midlatitude storms towards the Antarctic periphery and lead to dry conditions at midlatitudes, including northern Patagonia (Gillett et al., 2006). The positive SAM trend is a consequence of both an increase in greenhouse gases in the troposphere and the depletion of ozone in the stratosphere. Climate models consistently project a continuation of a positive-phase SAM and therefore continued drought in western Patagonia for decades to come (Aguayo et al., 2019).

Extreme drought over Patagonia (as observed in austral summer 2021), requires additional forcing, such as the one often provided by the ENSO and natural variations in the SAM (Garreaud, 2018). In 2021, the ENSO was in a La Niña phase, which often results in a slightly higher than usual summer rainfall. The intense drought and strong southerly winds in Patagonia were then largely driven by the SAM positive-phase, including highly positive pressure anomalies over the midlatitude SE Pacific (Fig. 2A). Interestingly, the positive-phase SAM in austral summer-fall 2021 occurred simultaneously with a massive ozone hole that had developed over Antarctica during the previous spring (September–October 2020). Although the ENSO and SAM involved disparate vertical levels (the lower troposphere and mid stratosphere), they were, nonetheless, dynamically connected (Lim et al., 2019) and provided some degree of predictability for summer drought in north Patagonia as well as for the potential development of HABs.

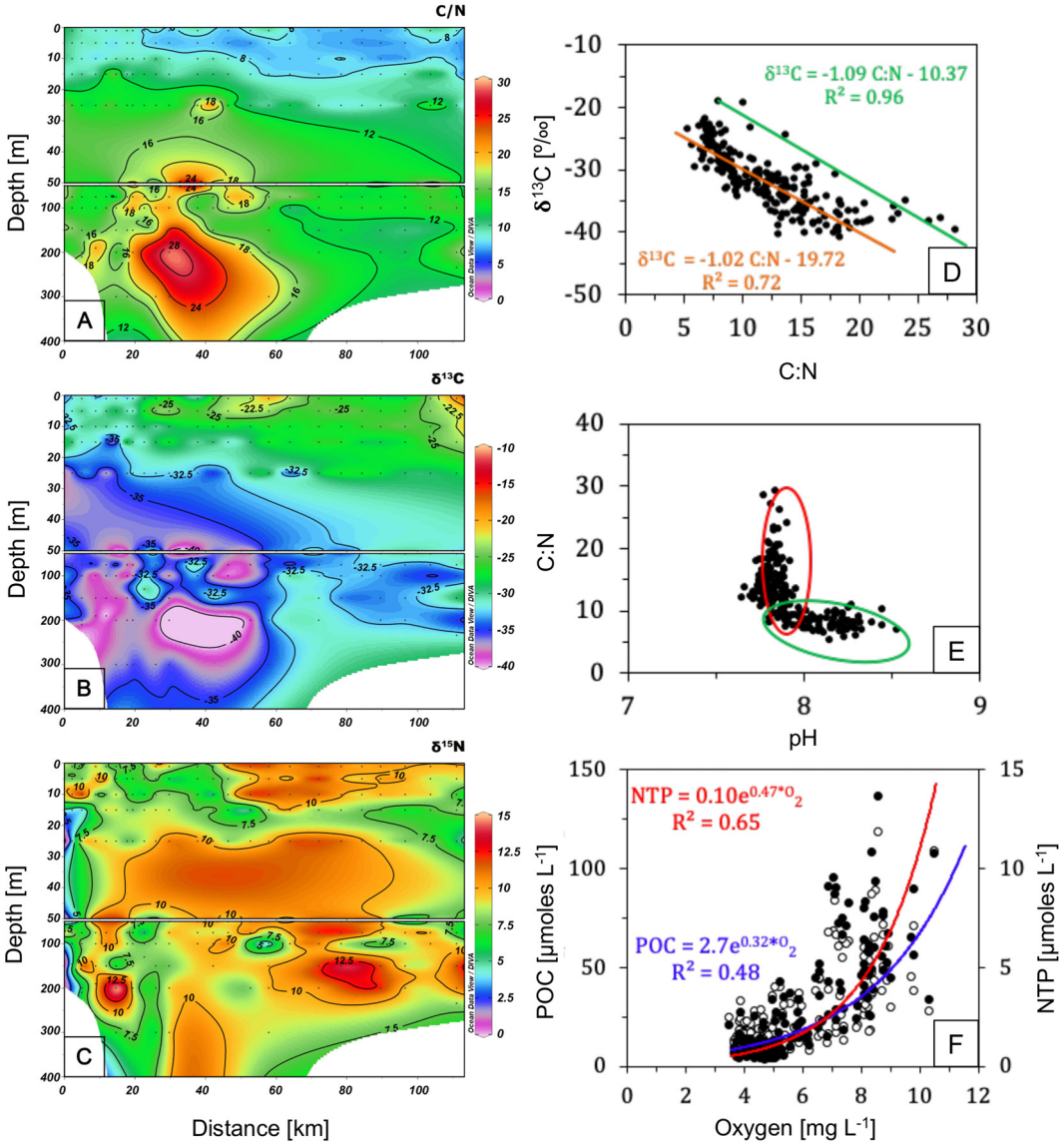

Fig. 9. A) Molecular C:N ratio; B) isotopic signals of particulate organic carbon ($\delta^{13}C_{POC}$, ‰) and C) particulate organic nitrogen ($\delta^{15}N_{TN}$, ‰); D) relation between the isotopic signal of carbon vs the C:N ratio. Linear regression equation for the surface samples (green) and deep samples (orange); E) Relation between the C:N ratio and pH in samples at 30 m (green ellipse) and below (red ellipse); F) exponential relation between particulate organic carbon (POC, µmol L^{-1}) and nitrogen (PON, µmol L^{-1}) and the dissolved oxygen concertation (mg L^{-1}). Exponential relation of POC vs. O2 (violet) and PON vs. O2 (red). (For interpretation of the references to colour in this figure legend, the reader is referred to the web version of this article.)

4.2. Physical-chemical and biological drivers of bloom development

The chronology of the development of water masses along Comau Fjord during the study period was characterized by a seasonal variation that allowed the continuous exchange of estuarine and oceanic water (Fig. 6 and Fig. S2) (Fillinger and Richter, 2013; García-Herrera et al., 2022). The vertical distribution of absolute salinity was indicative of the entrance of oceanic water, i.e., SAAW, during March 2021 (Fig. 6). While the contribution of this water mass was initially 18.3 %, it increased to 70 % in winter 2021 (Fig. S2). The salinity data from March 2021 highlighted the upward movement of the isohaline of 33 g kg^{-1} at the fjord head zone. Inorganic nutrients (Fig. 7) followed the same response as salinity, providing further evidence of a local upwelling process.

Recently, Crosswell et al. (2022) reported the presence of a local upwelling in the head zone of Reloncaví Fjord, due to the influence of down-fjord winds. The upwelling was cited as one of the main factors contributing to the input of nutrient-rich water into the euphotic layer, in turn favoring primary production. Additional mechanisms contributing to the mixing processes were synoptic winds (mainly from the north and produced by a low atmospheric pressure system) and the katabatic (southerly) winds in Comau Fjord. Favorable upwelling winds were also reported in the northern Patagonian fjords during spring-summer, owing to the southern migration of the southeast Pacific subtropical anti-cyclone. A spring-summer dominance of the wind regime by southerly winds was determined as well (Narváez et al., 2019; Pérez-Santos et al., 2019). The favorable upwelling winds at the head of Comau Fjord contributed to the *H. akashiwo* bloom in March 2021. As the southerly low-level winds over this area in summer 2021 were the strongest on record (Fig. 2D), they would have played a key role in HAB development.

Double-diffusive convection (DDC) also promoted a mixing of the water column in the Patagonian fjords and channels (Pérez-Santos et al., 2014). A quantification of the DDC in Patagonian waters revealed two different processes: diffusive-layering and salt fingering, accounting for 40 % and 1 % of the total data, respectively. In general, the change in sign of the vertical

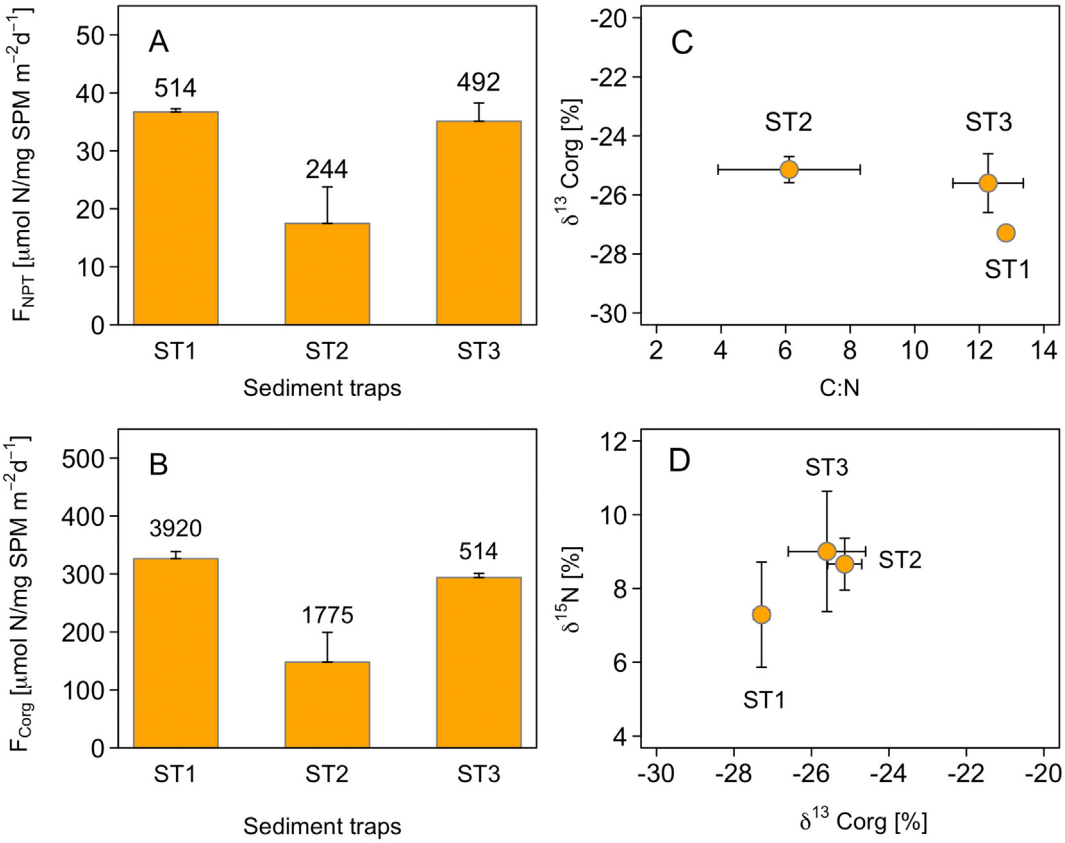

Fig. 10. Fluxes of organic matter: A) Nitrogen and B) carbon (µmol per mg of SPM sedimented m^{-1} day^{-1} for three sediment traps located at three stations, representing the head (ST1), middle (ST2), and mouth (ST3) of Comau Fjord. Numbers over the bar indicate mg of N or C. C) Relation of the isotopic signal of carbon ($\delta^{13}C_{POC}$, ‰) vs. the molecular ratio of C:N. D) Relation between isotopic signals of nitrogen ($\delta^{15}N_{PN}$, ‰) and carbon ($\delta^{13}C_{POC}$, ‰).

gradients of the temperature and salinity profiles in the water column contributed to the origin of processes such as the diffusive layering/salt fingering events that take place when temperature and salinity increase/decrease with depth (You, 2002). Salt fingering occurs when warmer, salty water overlaps colder, less salty water (Kelley et al., 2003). Data collected during an oceanographic cruise in Comau Fjord in March 2018 registered salt fingering events in the euphotic layer (15–30 m), and was postulated to be a significant process controlling metabolism in the waters of Comau Fjord (Crosswell et al., 2022). A quantitative analysis of DDC in Comau Fjord during March 2021 revealed the presence of salt fingering events at depths of 100–200 m (Fig. S3). This mixing process in the water column of the fjord head zone occurred in the same layer as the upward movement of salinity and inorganic nutrients, eventually resulting in the entrance of nutrients into the euphotic layer, which in turn gave rise to the intense bloom.

The strong southerly winds that favored upwelling and salt-fingering could additionally have induced the resuspension of microalgal cysts in the water column at the head of Comau Fjord. Several studies have pointed out that the frequent recurrence of many HAB species in certain areas, including eastern boundary upwelling systems, can be linked to the presence of seedbeds (Pitcher and Louw, 2021; Trainer et al., 2010). Recent investigations of sediments from aquaculture farms revealed the presence of cysts of several modern dinocysts, and therefore of seedbanks for HAB efflorescences (Balaji-Prasath et al., 2022). Although we did not find evidence of the presence of *H. akashiwo* resting cysts in the sediments of Patagonian fjords and channels, an examination of sediments in Northwestern Patagonia showed that they harbored cysts of many HAB species, including those known to be toxigenic, albeit at varying densities and with different environmental implications (Rodríguez-Villegas et al., 2022a).

H. akashiwo enters a resting stage when conditions are not suitable for its vegetative growth (Itakura et al., 1996; Kim et al., 2015). Resting stages are characterized by metabolic stasis and allow survival in the sediments until either bottom conditions or resuspension events permit germination, in which case the cysts enter a vegetative, proliferative stage that allows bloom development. The rapid formation of cysts under nutrient limitation is enabled by a direct shift from a vegetative to a dormant stage, mediated by an asexual life cycle stage, such that gamete and zygote formation is bypassed (Han et al., 2002). The germination of *H. akashiwo* cysts is likewise very fast, as it is constrained only by environmental factors, mostly temperature and light, without a mandatory cyst maturation period. For other raphidophyte species, germination requires several months (see for example Imai and Yamaguchi, 2012). The temperature threshold for germination is 10 °C (Imai and Itrakura, 1999) and the light requirement is very low (5 µmol photons m^{-2} s^{-1}) (Han et al., 2002). The presence of cysts of *H. akashiwo* and the environmental dynamics of their germination in Japan were previously studied and temperature and light were shown to affect cyst germination, although whether they also regulate natural seedbanks is not well understood (Imai and Itrakura, 1999; Shikata et al., 2007).

The *H. akashiwo* bloom that occurred in September 1988 coincided with a Marine Heat Wave (MHW) in northern Chilean Patagonia, during which the sea surface temperature increased by 0.6 °C (Pujol et al., 2022), sufficient to promote the growth of *H. akashiwo* (Sandoval-Sanhueza et al., 2022). During that bloom event, cell densities up to 1×10^5 cells mL^{-1} were detected in the inner sea of Chiloé, with resting cysts as the most likely source of the initial microalgal inoculum. An uplift together with the marine topography of the affected zone, which includes submarine canyons, could have promoted the resuspension of microalgal benthic resting stages from waters as deep as 200 m into the photic zone, where if the temperature

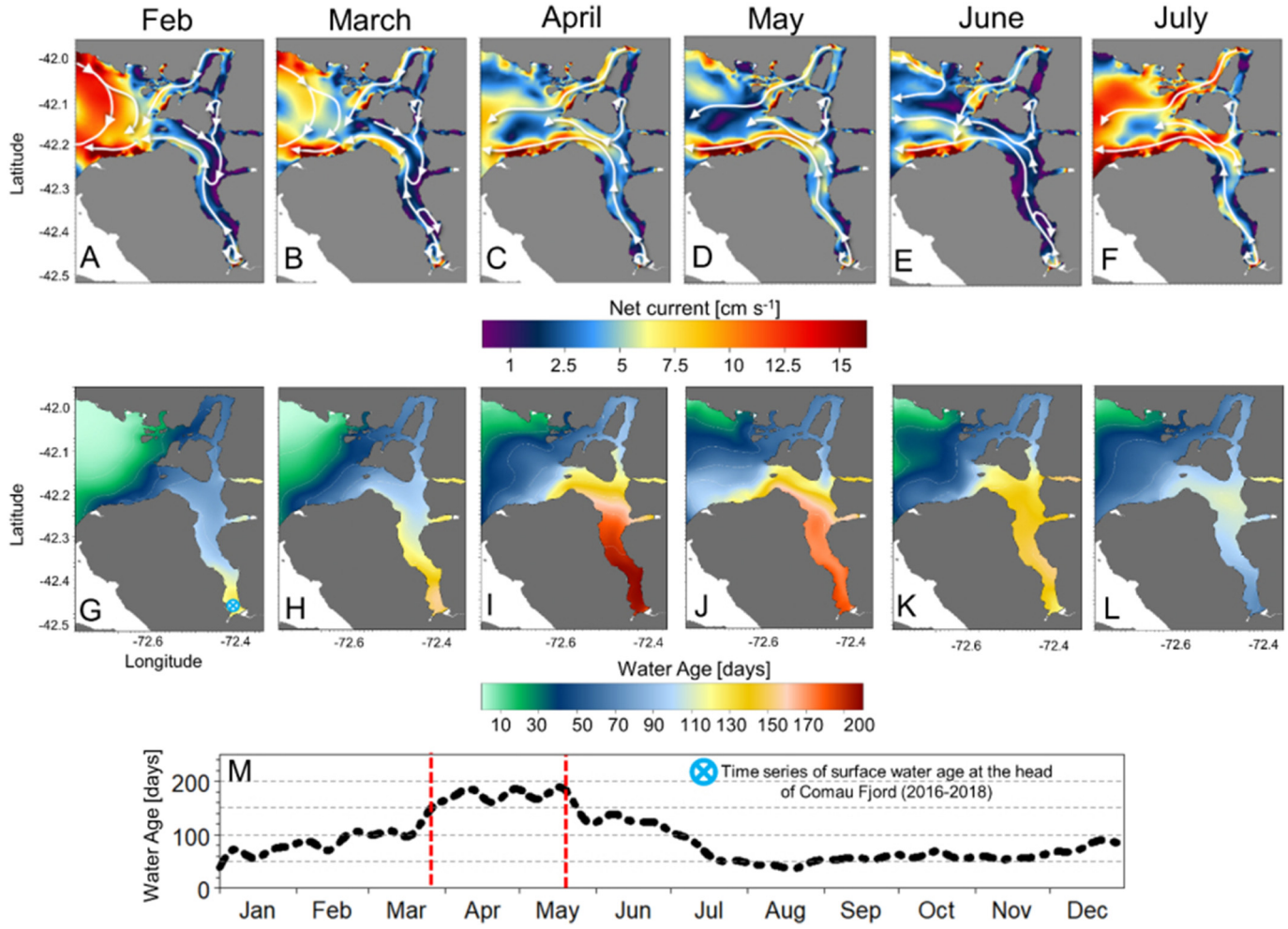

Fig. 11. Monthly mean circulation pattern (A–F) and mean water age (G–L) for the surface layer (0–10 m) during February to July (2016–2018). M) Time series of water age at the head of Comau Fjord in the surface layer (0–10 m). The red dashed line indicates the period of annual maximum water age. (For interpretation of the references to colour in this figure legend, the reader is referred to the web version of this article.)

allowed, germination would have been possible (Rodríguez-Villegas et al., 2022b). The combined impact of upwelling winds and salt fingering on seedbanks of *H. akashiwo* in Comau Fjord needs to be further studied to understand whether these same conditions promote recurrent blooms of this species.

4.3. Circulation pattern and bloom retention

Comau Fjord is a deep estuarine system with a sill at its mouth (Fig. 1C) that separates the inner basin of 470 m from the outer basin of 300 m. Consequently, deep water below 300 m remains stagnant for long periods of the year (Fig. 12). An analysis of water age via a simulation in our hydrodynamic model revealed that, from spring to summer, deep water gradually becomes isolated from an exchange with water outside of the fjord, due to a blockage at the sill (between 100 and 300 m), resulting in older water in the deep layer during this period. In the fall, when the deep layer reaches its maximum age (220 days), an intrusion of outer water in the intermediate layer causes a strong uplift of the resident water at the fjord's head, transporting it to the shallower layer, where it remains for 200 days. Water in the deep basin, however, is renewed in the fall, due to the intrusion of denser water that flushes the fjord at its deep and intermediate layers with an outflow that is accentuated in winter, resulting in a water age of only 50 days.

The water renewal mechanism causes resident water in the deep basin to rise towards the surface. Thus, water renewal events during the early fall appear to directly trigger the uplift of older, stagnant water, first in the intermediate layer and then in the deep layer (Fig. 12). This sinking process occurs when the density of the intrusive water is higher than that of the resident water in the deep layer (Gade and Edwards, 1980), as determined from the CTD-based salinity profiles showing a 33-isohaline uplift at Comau Fjord, particularly during May and June (Fig. S1).

Prior to renewal events in the deep layer, surface (upper 10 m) circulation is slow, with gyres at both the mouth and head of the fjord, causing water retention. Surface water reached its maximum age (200 days) towards the head in early fall, indicating active uplift due to water replenishment in deeper layers (Fig. 11). This uplift likely transported nutrients from the deep layer to the shallow photic zone of the fjord's basins, in turn triggering the phytoplankton bloom (Jonsson et al., 2009; Sutula et al., 2017; Watts et al., 1998; Watts, 1994). Based on observational evidence, Salamena et al. (2022) proposed a role for deep-water renewal in triggering phytoplankton blooms in a tropical shallow water fjord (Ambon Bay, Indonesia). Deep-water intrusions in the fjords of Ambon Bay were shown to cause an uplift of nutrient-rich resident deep water, resulting in its displacement to the surface (Salamena et al., 2022).

The results of the models indicated that this uplift mechanism occurs annually, but the ability of deeper, more saline, and nutrient-rich waters to reach the top few meters of the water column may depend on other factors as well. According to the results of these same models (not shown), a larger volume of saline water ascended to shallower layers in the fall of 2016, when river discharges were below-average, than was the case in the autumn of 2017 or 2018, such that discharges were near or above average.

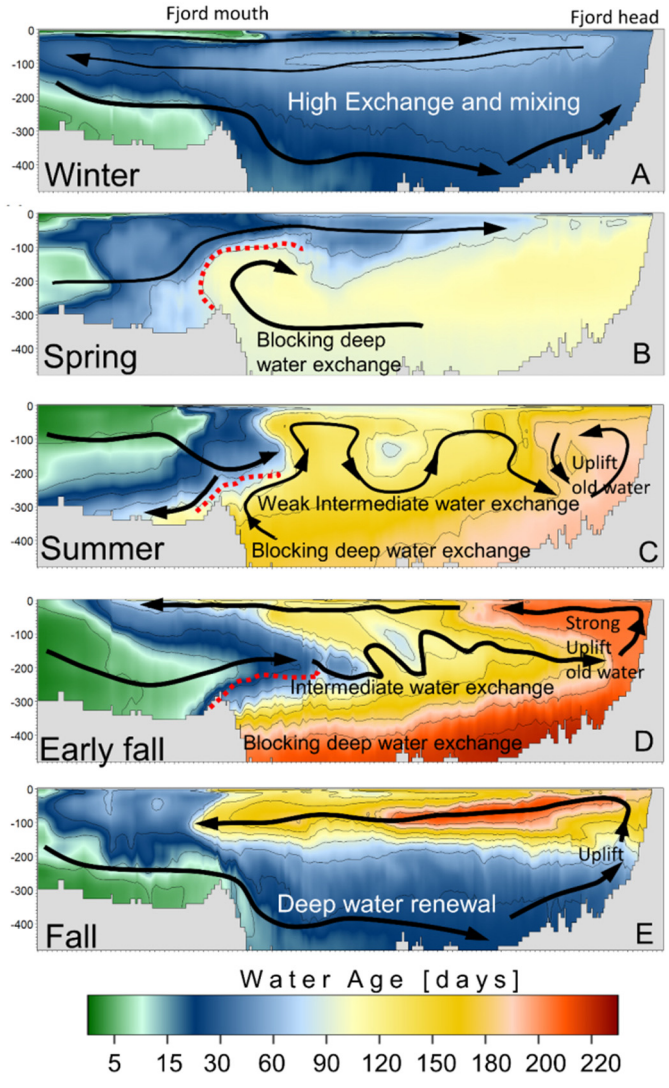

Fig. 12. Water age along Comau Fjord in A) winter, B) spring, C) summer, D) early fall and E) fall of 2016–2018.

This implies that the strength of the freshwater layer prevents the ascent of older, more saline, and nutrient-rich waters to the surface. Further studies are required to update the modelling periods for the 2021 event and thus determine whether the simulations accurately reproduced this process.

4.4. Biogeochemical conditions during the HAB event

Biogeochemical analyses showed that nitrate, phosphate, SPM, Chl-a, POC, and PON concentrations were highest in the upper water layer in summer, with high concentrations measured at the head of the fjord, where the bloom of *H. akashiwo* initiated. C:N values were high throughout the water column, with a nucleus of maximal values in the middle layer at the head of the fjord, whereas silicates were homogeneously distributed in the deep water layer, with maximal values reached in autumn. The Redfield ratios and isotopic values of C and N clearly indicated an excess of organic C, including its enrichment in the surface waters from the head to the mouth of the fjord and an enrichment of TN throughout the water column. Compared to the expected Redfield value (6.625), which is based on the molar relationship between C and N for phytoplankton (106:16), the value of the slope was slightly higher, due to the carbon excess of ~57.5 μg L^{-1} (4.58 mol). PON and POC concentrations were highest inside the fjord and decreased with depth. The biogeochemical dynamics showed that a decreasing pH gradient correlated with an increasing C:N ratio, while DO correlated positively with PON, but not with POC, in an exponential relationship. Organic matter fluxes in the fjord sediment showed differences between the head and the rest of the fjord.

These results provide strong evidence that an unusual upwelling of acidic, nutrient-rich waters to the surface layer favored the development of the *H. akashiwo* bloom at the head of the fjord and then sustained the bloom throughout the fjord during the summer-autumn of 2021, thus coinciding with a La Niña phase. The formation of HABs in upwelling systems around the world is well documented and the dynamics of these events have been investigated in large-scale studies (Capone and Hutchins, 2013; Díaz et al., 2016; Feely et al., 2008; Kudela et al., 2010; Pitcher et al., 2010; Pitcher and Louw, 2021; Trainer et al., 2010). The role played by nitrates, phosphates, and silicates in the growth of HAB species has been convincingly demonstrated in several laboratory studies (reviewed in Lin et al., 2016). However, field studies of the dynamics that govern the role of nutrients during bloom initiation and maintenance are rare. In a recent metatranscriptomic study from the East China Sea, *H. akashiwo* was shown to rapidly take up and utilize inorganic P during bloom initiation and to up-regulate the expression of genes related to mixotrophy during the bloom peak, consistent with the use of organic C from mixotrophy to sustain the high concentration of cells forming the bloom (Ji et al., 2018). These results are in agreement with those of the current study and provide further evidence that high levels of N, P, and organic C from upwelling waters contributed to the initiation and subsequent maintenance of the *H. akashiwo* bloom in Comau Fjord in March 2021.

4.5. Future perspectives

Prognostic climate models consistently project a continuation of a positive-phase SAM, in which case the drought in western Patagonia can be expected to worsen over the coming decades. The decrease in river discharge will affect the strength of the surface estuarine layer, which prevents the ascent of older, more saline and nutrient-rich waters to the first few meters of the water column, thus facilitating density stratification near the water surface. The latter plays an important role in the generation and maintenance of microalgal blooms, as demonstrated in Comau Fjord. Moreover, as suggested by the models generated in this study, the reproduction of this sequence of events in fjords characterized by high turnover rates and high nutrient concentrations would increase their risk of HABs as well.

5. Conclusions

An exceptional HAB event caused by *H. akashiwo* occurred during March 2021 in Comau Fjord, Chilean Patagonia, resulting in enormous losses of farmed salmon. Taking advantage of a phytoplankton monitoring program and oceanographic data, we analyzed the development and evolution of the bloom in relation to its physical-chemical dynamics and climatic-hydrological-oceanographic drivers. Changes in the water column during the bloom were evaluated using a hydrodynamic model that included water renewal. This multi-faceted approach, the product of a collaboration between public (universities and institutes) and private (salmon farm) sectors, provided insights into the bloom dynamics of *H. akashiwo*, one of the most widespread ichthyotoxic HAB species in the world. This knowledge is essential in efforts to reduce, if not prevent, the large-scale mortality of wild and farmed fish species in northern Patagonian fjords. Our study also introduced several useful tools for the better management and protection of deep-sea coral ecosystems and their unique biodiversity, which globally are under strong natural and anthropogenic pressure.

A persistent anticyclone over the southern tip of the continent, in connection with the positive SAM phase, was hypothesized to be one of the main climate drivers of the extreme drought over Patagonia. These conditions accounted for a reduced cloud cover and thus a high level of solar radiation reaching the fjord, resulting in a warming of the surface layer (18 °C). The higher temperature and the injection of nutrient-rich waters,

possibly carrying microalgal resting stages, favored bloom formation. The same anticyclonic anomaly responsible for the temperature increase forced strong southerly winds (the strongest on record) over northern Patagonia, fostering an upwelling at the head of Comau Fjord. The resulting upward shift at the fjord head zone promoted the injection of inorganic nutrients into the euphotic layer. The hydrodynamic model demonstrated the significance of water renewal in Comau Fjord via uplifts of deep water to the surface layer, a process that would also promote the resuspension of benthic resting stages of HAB species and their ascent into the photic layer, especially at the fjord head. Salt-fingering events in the same layer as the upwelling enhanced mixing within the water column and therefore the transport of nutrients to the layer where *H. akashiwo* developed. Two months after this HAB event, the signals from the subsurface layer of Comau Fjord were still those of the bloom, including the expansion of low-DO water and a significant increase in inorganic nutrients due to the recycling processes occurring during organic matter degradation. The biogeochemical parameters (POC, DOC, C:N ratio, and stables isotopes of $\delta^{13}C$ and $\delta^{15}N$) confirmed the large inputs carbon and nitrogen into the fjord during this bloom.

CRediT authorship contribution statement

Patricio A. Díaz: Conceptualization, Methodology, Software, Validation, Formal analysis, Investigation, Resources, Writing – original draft, Writing – review & editing, Visualization, Supervision. **Iván Pérez-Santos:** Conceptualization, Methodology, Formal analysis, Investigation, Resources, Writing – original draft, Writing – review & editing, Visualization, Project administration, Funding acquisition. **Leila Basti:** Conceptualization, Methodology, Validation, Formal analysis, Investigation, Writing – original draft, Writing – review & editing. **René Garreaud:** Conceptualization, Methodology, Software, Validation, Formal analysis, Investigation, Resources, Writing – original draft, Writing – review & editing, Visualization. **Elias Pinilla:** Conceptualization, Methodology, Software, Validation, Formal analysis, Resources, Writing – original draft, Writing – review & editing, Visualization. **Facundo Barrera:** Conceptualization, Methodology, Software, Validation, Formal analysis, Resources, Writing – original draft, Writing – review & editing, Visualization. **Alfredo Tello:** Resources, Writing – original draft, Writing – review & editing, Visualization, Supervision. **Camila Schwerter:** Methodology, Software, Formal analysis, Investigation, Writing – original draft, Writing – review & editing, Visualization. **Sara Arenas-Uribe:** Methodology, Software, Formal analysis, Investigation, Writing – original draft, Writing – review & editing, Visualization. **Camila Soto-Riquelme:** Methodology, Software, Formal analysis, Investigation, Writing – review & editing, Visualization. **Pilar Navarro:** Software, Formal analysis, Investigation, Visualization. **Manuel Díaz:** Software, Formal analysis, Investigation, Visualization. **Gonzalo Álvarez:** Conceptualization, Methodology, Validation, Formal analysis, Investigation, Writing – original draft, Writing – review & editing, Visualization. **Pamela M. Linford:** Software, Formal analysis, Investigation, Visualization. **Robinson Altamirano:** Methodology, Investigation, Writing – review & editing, Visualization. **Guido Mancilla-Gutiérrez:** Methodology, Investigation, Writing – review & editing, Visualization. **Camilo Rodríguez-Villegas:** Methodology, Investigation, Writing – review & editing, Visualization. **Rosa I. Figueroa:** Conceptualization, Methodology, Investigation, Resources, Writing – original draft, Writing – review & editing, Visualization, Supervision.

Data availability

Data will be made available on request.

Declaration of competing interest

The authors declare that they have no known competing financial interests or personal relationships that could have appeared to influence the work reported in this paper.

Acknowledgements

We thank Cesar Salgado (*R.V. Jürgen Winter* captain) for technical assistance during the cruises; the Chonos initiative of the Instituto de Fomento Pesquero (IFOP) for facilitating the use of its computer systems to access the MIKE 3, WRF and FLOW models; and the Ministry of Economy, Development and Tourism of the Chilean Government for funding through the Undersecretary of Fisheries and Aquaculture. Patricio A. Díaz was funded by Centre for Biotechnology and Bioengineering (CeBiB) (PIA project FB0001, ANID, Chile). Iván Perez-Santos was funded by COPAS Sur-Austral (ANID AFB170006), COPAS COASTAL (ANID FB210021), CIEP R20F002, and FONDECYT 1211037. Rosa I. Figueroa was funded by a national project from the Spanish Ministry of Science and Innovation and the European Community, European Regional Development Fund (ERDF; Project DIANAS-CTM2017-86066-R) and a grant from the Galician Networks of Excellence (GRC-VGOHAB IN607A-2019/04) of the Innovation Agency of the Xunta de Galicia (GAIN). Elias Pinilla acknowledges funding from the National Science Foundation (NSF grant number 2045866), which peripherally contributed to the work conducted for this study. We are grateful to the two reviewers for constructive criticism that helped to improve the manuscript.

Appendix A. Supplementary data

Supplementary data to this article can be found online at https://doi.org/10.1016/j.scitotenv.2022.161288.

References

Aguayo, R., León-Muñoz, J., Vargas-Baecheler, J., Montecinos, A., Garreaud, R., Urbina, M., et al., 2019. The glass half-empty: climate change drives lower freshwater input in the coastal system of the Chilean Northern Patagonia. Clim. Chang. https://doi.org/10.1007/s10584-019-02495-6.

Álvarez, G., Díaz, P.A., Godoy, M., Araya, M., Ganuza, I., Pino, R., et al., 2019. Paralytic shellfish toxins in *Mesodesma donacium* during an exceptional bloom of *Alexandrium catenella* associated to an intense mass mortality. Toxins 11, 188.

Álvarez-Garreton, C., Mendoza, P.A., Boisier, J.P., Addor, N., Galleguillos, M., Zambrano-Bigiarini, M., et al., 2018. The CAMELS-CL dataset: catchment attributes and meteorology for large sample studies – Chile dataset. Hydrol. Earth Syst. Sci. 22.

Avaria, S., Cáceres, M., Muñoz, P., Palma, S., Vera, P., 1999. Plan nacional sobre floraciones de algas nocivas en Chile, p. 31 Valparaiso, Chile.

Balaji-Prasath, B., Wang, Y., Su, Y.P., Lin, H., Feng, S., Zheng, L., 2022. Distribution of dinoflagellate cysts in the modern sediments from the coastal aquaculture area and its adjacent oceanic shelf southest China. Reg. Stud. Mar. Sci. 55, 102502.

Barrera, F., Lara, R.J., Krock, B., Garzón Cardona, J.E., Fabro, E., Koch, B.P., 2017. Factors influencing characteristics and distribution of organic particles and macromolecules in the Pacific-Atlantic connection. J. Mar. Syst. 175, 36–45.

Basti, L., Nagai, K., Go, J., Okano, S., Oda, T., Tanaka, Y., et al., 2016. Lethal effects of ichthyotoxic raphidophytes, *Chattonella marina*, *C. antiqua*, and *Heterosigma akashiwo*, on post-embryonic stages of the Japanese pearl oyster, *Pinctada fucata martensii*. Harmful Algae 59, 112–122.

Basti, L., Go, J., Okano, S., Higuchi, K., Nagai, S., Nagai, K., 2021. Sublethal and antioxidant effects of six ichthyotoxic algae on early-life stages of Japanese pearl oyster. Harmful Algae 103, 102013.

Bianchi, T.S., 2007. Biogeochemistry of Estuaries. Oxford University Press, New York, NY.

Boisier, J.P., Alvarez-Garreton, C., Cordero, R.R., Damiani, A., Gallardo, L., Garreaud, R., et al., 2018. Anthropogenic drying in central-southern Chile evidenced by long-term observations and climate model simulations. Elementa 6, 74.

Bolin, B., Rodhe, H., 1973. A note on the concepts of age distribution and transit time in natural reservoirs. Tellus 25, 58–62.

Burkholder, J.M., 1998. Implication of harmful microalgae and heterotrophic dinoflagellates in management of sustainable marine fisheries. Ecol. Appl. 8, S37–S62.

Calvete, C., Sobarzo, M., 2011. Quantification of the surface brackish water layer and frontal zones in southern Chilean fjords between Boca del Guafo (43°30′S) and Estero Elefantes (46°30′S). Cont. Shelf Res. 31, 162–171.

Capone, D.G., Hutchins, D.A., 2013. Microbial biogeochemistry of coastal upwelling regimes in a changing oceean. Nat. Geosci. 6, 711–717.

Clément, A., Aguilera, A., Fuentes, C., 2002. Análisis de la Marea Roja en el Archipiélago de Chiloé, Contingencia verano 2002. XXII Congreso de Ciencias del Mar Universidad Austral de Chile, Valdivia, Chile.

Clément, A., Lincoqueo, L., Saldivia, M., Brito, C.G., Muñoz, F., Fernández, C., et al., 2016. Exceptional summer conditions and HABs of *Pseudochattonella* in southern Chile create record impacts on salmon farm. Harmful Algae News 53, 1–3.

Clément, A., Muñoz, F., Correa, N., Ramírez, N., Cresinim, R., Brito, C.G., et al., 2021. Fish killer *Heterosigma akashiwo* in Comau Fjord, Southern Chile. Harmful Algae News 68, 7–8.

Crosswell, J.R., Bravo, F., Pérez-Santos, I., Carlin, G., Cherukuru, N., Schwarger, C., et al., 2022. Geophysical controls on metabolic cycling in three Patagonian fjords. Prog. Oceanogr. 207, 102866.
Delhez, E.J.M., Campin, J.M., Hirst, A.C., Deleersnijder, E., 1999. Toward a general theory of the age in ocean modelling. Ocean Model. 1, 17–27.
DHI, 2019. Mike 3, User Guide and Reference Manual. Danish Hydraulic Institute, Denmark.
Díaz, P.A., Molinet, C., Seguel, M., Díaz, M., Labra, G., Figueroa, R., 2014. Coupling planktonic and benthic shifts during a bloom of *Alexandrium catenella* in southern Chile: implications for bloom dynamics and recurrence. Harmful Algae 40, 9–22.
Díaz, P.A., Ruiz-Villarreal, M., Pazos, Y., Moita, M.T., Reguera, B., 2016. Climate variability and *Dinophysis acuta* blooms in an upwelling system. Harmful Algae 53, 145–159.
Díaz, P.A., Álvarez, A., Varela, D., Pérez-Santos, I., Díaz, M., Molinet, C., et al., 2019. Impacts of harmful algal blooms on the aquaculture industry: Chile as a case study. Perspect. Phycol. 6, 39–50.
Díaz, P.A., Pérez-Santos, I., Álvarez, G., Garreaud, R., Pinilla, E., Díaz, M., et al., 2021. Multiscale physical background to an exceptional harmful algal bloom of *Dinophysis acuta* in a fjord system. Sci. Total Environ. 773, 145621.
Díaz, P.A., Álvarez, G., Pizarro, G., Blanco, J., Reguera, B., 2022a. Lipophilic toxins in Chile: history, producers and impacts. Mar.Drugs 20, 122.
Díaz, P.A., Molinet, C., Seguel, M., Niklitschek, E.J., Díaz, M., Álvarez, G., et al., 2022b. Modelling the spatial and temporal dynamics of paralytic shellfish toxins (PST) at different scales: implications for research and management. Toxins 14, 786.
Edvardsen, B., Imai, I., 2006. The ecology of harmful flagellates within Prymnesiophyceae and Raphidophyceae. In: Granéli, E., Turner, J.T. (Eds.), Ecology of Harmful Algae. Ecological Studies (Analysis and Synthesis). 189. Springer, Berlin, Heidelberg.
FAO, 2016. GLOBEFISH - Analysis and Information on World Fish Trade.
Feely, R., Chris, S., Hernández-Ayon, J.M., Ianson, D., Hales, B., 2008. Evidence for upwelling of corrosive "acidified" water onto the continental shelf. Science 320, 1490–1492.
Fillinger, L., Richter, C., 2013. Vertical and horizontal distribution of *Desmophyllum dianthus* in Comau Fjord, Chile: a cold-water coral thriving at low pH. PeerJ 1, e194.
Fogt, R.L., Marshall, G.J., 2020. The southern annular mode: variability, trends, and climate impacts across the Southern Hemisphere. WIREs Clim. Chang. 11, e652.
Försterra, G., Häussermann, V., Laudien, J., Jantzen, C., Sellanes, J., Muñoz, P., 2014. Mass die-off of the cold-water coral *Desmophyllum dianthus* in the Chilean Patagonian fjord region. Bull. Mar. Sci. 90, 895–899.
Fuentes, C., Clement, A., Aguilera, A., 2008. Summer *Alexandrium catenella* bloom and the impact on fish farming en the XI Aysén region, Chile. In: Moustrup, O., Doucette, G., Enevoldsen, H., Godhe, A., Hallegraeff, G., Luckas, B., et al. (Eds.), Proceeding of the International Conference on Harmful Algae. International Society for the Study of Harmful Algae and Intergovernmental Oceanographic Commission of UNESCO, Copenhagen, pp. 183–186.
Gade, H.D., Edwards, A., 1980. Deep water renewal in fjords. In: Freeland, H.J., Farmer, D.M., Levings, C.D. (Eds.), Fjord Oceanography. Springer, US, Boston, MA, pp. 453–489.
García-Herrera, N., Cornils, A., Laudien, J., Niehoff, B., Höfer, J., Försterra, G., et al., 2022. Seasonal and diel variations in the vertical distribution, composition, abundance and biomass of zooplankton in a deep Chilean Patagonian Fjord. PeerJ 10, e12823.
Garreaud, R., 2007. Precipitation and circulation covariability in the extratropics. J. Clim. 20, 4789–4797.
Garreaud, R., 2018. Record-breaking climate anomalies lead to severe drought and environmental disruption in western Patagonia in 2016. Clim. Res. 74, 217–229.
Garreaud, R., Clem, K., Veloso, J.V., 2021. The South Pacific pressure trend dipole and the southern blob. J. Clim. 34, 7661–7676.
Gillett, N.P., Kell, T.D., Jones, P.D., 2006. Regional climate impacts of the southern annular mode. Geophys. Res. Lett. 33, L23704.
Glibert, P.A., 2020. Harmful algae at the complex nexus of eutrophication and climate change. Harmful Algae 91, 101583.
Glibert, P.M., Anderson, D.M., Gentien, P., Granelí, E., Sellner, K.G., 2005. The global and complex phenomena of harmful algal blooms. Oceanography 18, 136–147.
Gobler, C.J., Doherty, O.M., Hattenrath-Lehamnn, T.K., Griffith, A.W., Kang, Y., Litaker, R.W., 2017. Ocean warming since 1982 has expanded the niche of toxic algal blooms in the North Atlantic and North Pacific oceans. Proc. Natl. Acad. Sci. U. S. A. 114, 4975–4980.
González, H.E., Nimptsch, J., Giesecke, R., Silva, N., 2019. Organic matter distribution, composition and its possible fate in the Chilean North-Patagonian estuarine system. Sci. Total Environ. 657, 1419–1431.
Grasshoff, K., Ehrhardt, M., Kremling, K., 1983. Methods of Seawater Analysis. 2nd edition. Verlag Chemie Weinhein, New York, USA.
Grasshoff, K., Kremling, K., Ehrhardt, M., 1999. Methods of Seawater Analysis. Wiley-VCH, Weinheim, Germany.
Griffith, A.W., Gobler, C.J., 2020. Harmful algal blooms: a climate change co-stressor in marine and freshwater ecosystems. Harmful Algae 91, 101590.
Hallegraeff, G., 2003. Harmful algal bloom: a global overview. In: Hallegraeff, G., Anderson, D.M., Cembella, A.D. (Eds.), Manual on Harmful Marine Microalgae. Monographs on Oceanographic Methodology. UNESCO Publishing, France, pp. 25–50.
Hallegraeff, G.M., Anderson, D.M., Belin, C., Bottein, M.-Y.D., Bresnan, E., Chinain, M., et al., 2021. Perceived global increase in algal blooms is attributable to intensified monitoring and emerging bloom impacts. Commun.Earth Environ. 2, 117.
Han, M.-S., Kim, Y.-P., Cattolico, R.A., 2002. *Heterosigma akashiwo* (Raphidophyceae) resting cell formation in batch culture: strain identity versus physiological response. J. Phycol. 38, 304–317.
Haury, L.R., McGowan, J.A., Wiebe, P.H., 1978. Patterns and processes in the time-space scales of plankton distribution. In: Steele, J.H. (Ed.), Spatial Pattern in Plankton Communities. Springer Science, Plenum, New York, pp. 277–327.
Häussermann, V., Försterra, G., 2009. Fauna Marina Bentónica de la Patagonia Chilena. Nature in Focus, Santiago, Chile.
Holm-Hansen, Lorenzen C.J., Holmes, R.W., Strickland, J.D.H., 1965. Fluorometric determination of chlorophyll. J. Cons. Perm. Int. Explor. Mer. 30, 3–15.
Imai, I., Itrakura, S., 1999. Importance of cysts in the population dynamics of the red tide flagellate *Heterosigma akashiwo* (raphidophyceae). Mar. Biol. 133, 755–762.
Imai, I., Yamaguchi, M., 2012. Life cycle, physiology, ecology and red tide occurrences of the fish-killing raphidophyte *Chattonella*. Harmful Algae 14, 46–70.
IOC, SCOR, IAPSO, 2010. The International Thermodynamic Equation of Seawater - 2010: Calculation and Use of Thermodynamic Properties, Manual and Guides No. 56. (English), available from:Intergovernmen- tal Oceanographic Commission, UNESCO. http://www.TEOS-10.org.
Itakura, S., Nagasaki, K., Yamaguchi, M., Imai, I., 1996. Cyst formation in the red tide flagellate *Heterosigma akashiwo* (Raphidophyceae). J. Plankton Res. 18, 1975–1979.
Jantsen, C., Häussermann, V., Försterra, G., Laudrien, J., Ardelan, M., Maier, S., et al., 2013. Occurrence of a cold-water coral along natural pH gradients (Patagonia, Chile). Mar. Biol. 160, 2597–2607.
Ji, N., Lin, J., Li, L., Yu, L., Zhang, Y., Luo, H., et al., 2018. Metatransciptome analysis reveals environmental and diel regulation of *Heterosigma akashiwo* (raphyidophyceae) bloom. Appl.Microbiol.Int. 20, 1078–1094.
Jonsson, P.R., Pavia, H., Toth, G., 2009. Formation of harmful algal blooms cannot be explained by allelopathic interactions. Proc. Natl. Acad. Sci. U. S. A. 106, 11177–11182.
Kalnay, E., Kanamitsu, M., Kistler, R., Collins, W., Deaven, D., Gandin, L., et al., 1996. The NMC/NCAR 40-year reanalysis project. Bull. Am. Meteorol. Soc. 77, 437–471.
Kattner, G., Becker, H., 1991. Nutrients and organic nitrogenous compounds in the marginal ice zone of the Fram Strait. J.Mar.Syst. 2, 385–394.
Kelley, D.E., Fernando, H.J.S., Gargett, A.E., Tanny, J., Özsoy, E., 2003. The diffusive regime of double-diffusive convection. Prog. Oceanogr. 56, 461–481.
Khan, S., Arakawa, O., O'noue, Y., Cinneide, M., 1997. Neurotoxins in a toxic red tide of *Heterosigma akashiwo* (Raphidophyceae) in Kagoshima Bay, Japan. Aquac. Res. 28, 9–14.
Kim, D., Nakamura, A., Okamoto, T., Komatsu, N., Oda, T., Iida, T., et al., 2000. Mechanism of superoxide anion generation in the toxic red tide phytoplankton *Chattonella marina*: possible involvement of NAD(P)H oxidase. Biochim. Biophys. Acta, Gen. Subj. 1524, 220–227.
Kim, J.-H., Park, B.S., Wang, P., Kim, J.H., Youn, S.H., Han, M.-S., 2015. Cyst morphology and germination in *Heterosigma akashiwo* (Raphidophyceae). Phycologia 54, 435–439.
Kudela, R., Seeyave, S., Cochlan, W., 2010. The role of nutrients in regulation and promotion of harmful algal blooms in upwelling systems. Prog. Oceanogr. 85, 122–135.
Landsberg, J.H., 2002. The effects of harmful algal blooms on aquatic organisms. Rev. Fish. Sci. 10, 113–390.
León-Muñoz, J., Urbina, M.A., Garreaud, R., Iriarte, J.L., 2018. Hydroclimatic conditions trigger record harmful algal bloom in western Patagonia (summer 2016). Sci. Rep. 8, 1330.
Lim, E., Hendon, H., Butler, A., Thompson, D.W., Lawrence, Z., Scaife, A., et al., 2019. The 2019 Southern Hemisphere stratospheric polar vortex weakening and its impacts. Bull. Am. Meteorol. Soc. 102, E1150–E1171.
Lin, S., Liker, R.W., Sunda, W.G., 2016. Phosphorus physiological ecology and molecular mechanisms in marine phytoplankton. J. Phycol. 52, 10–36.
Lovegrove, T., 1960. An improved form of sedimentation apparatus for use with an inverted microscope. J.Cons.Permanent Int.Explor.Mer 25, 279–284.
Lucas, A.J., Largier, J.L., 2013. The influence of physical variability on HAB patterns and persistence in bays. In: GEOHAB, Roy, S., Pospelova, V., Montresor, M., Cembella, A. (Eds.), Global ecology and oceanography of harmful algal blooms, GEOHAB Core Research Project: HABs in fjords and coastal embayments. Second open science meeting: progress in interpreting life history and growth dynamics of harmful algal blooms in fjords and coastal environments. Intergovernmental Oceanographic Commission and Scientific Committee on Oceanic Research, Paris and Newark, DE, pp. 50–51 2013.
Maier, S.R., Jantzen, C., Laudien, J., Häussermann, V., Försterra, G., Cornils, A., et al., 2021. The carbon and nitrogen budget of *Desmophyllum dianthus* – a voracious cold-water coral thriving in an acidified Patagonian fjord. PeerJ 9, e12609.
Mardones, J.I., Clément, A., Rojas, X., Aparicio, C., 2010. *Alexandrium catenella* during 2009 in Chilean waters, and recent expansion to coastal ocean. Harmful Algae News 41, 8–9.
Mardones, J., Norambuena, L., Paredes-Mella, J., Fuenzalida, G., Dorantes-Aranda, J.J., Lee Chang, K.L., et al., 2020. Unraveling the *Karenia selliformis* complex with the description of a non-gymnodimine producing Patagonian phylotype. Harmful Algae 98, 101892.
Mardones, J.I., Paredes, J., Godoy, M., Suarez, R., Norambuena, L., Vargas, V., et al., 2021. Disentangling the environmental processes responsible for the world's largest farmed fish-killing harmful algal bloom: Chile, 2016. Sci. Total Environ. 766, 144383.
Meerhoff, E., Castro, L.R., Tapia, F.J., Pérez-Santos, I., 2019. Hydrographic and biological impacts of a glacial lake outburst flood (GLOF) in a Patagonian Fjord. Estuar. Coasts 42, 132–143.
Molinet, C., Lafón, A., Lembeye, G., Moreno, C.A., 2003. Patrones de distribución espacial y temporal de floraciones de *Alexandrium catenella* (Whedon & Kofoid) Balech 1985, en aguas interiores de la Patagonia noroccidental de Chile. Rev. Chil. Hist. Nat. 76, 681–698.
Monsen, N.E., Cloern, J.E., Lucas, L., Monismith, S.G., 2002. A comment on the use of flushing time, residence time, and age as transport time scales. Limmol.Oceanogr. 47, 1545–1553.
Narváez, D., Vargas, C., Cuevas, A., García-Loyola, S., Lara, C., Segura, C., et al., 2019. Dominant scales of subtidal variability in coastal hydrography of the Northern Chilean Patagonia. J. Mar. Syst. 193, 59–73.
Pantoja, S., Iriarte, J.L., Daneri, G., 2011. Oceanography of the Chilean Patagonia. Cont. Shelf Res. 31, 149–153.
Pérez-Santos, I., Garcés-Vargas, J., Schneider, W., Ross, L., Parra, S., Valle-Levinson, A., 2014. Double-diffusive layering and mixing in Patagonian fjords. Prog. Oceanogr. 129, 35–49.
Pérez-Santos, I., Seguel, R., Schneider, W., Linford, P., Donoso, D., Navarro, E., et al., 2019. Synoptic-scale variability of surface winds and ocean response to atmospheric forcing in the eastern austral Pacific Ocean. Ocean Sci.Discuss. 15, 1247–1266.
Pérez-Santos, I., Díaz, P.A., Silva, N., Garreaud, R., Montero, P., Henríquez-Castillo, C., et al., 2021. Oceanography time series reveals annual asynchrony input between oceanic and estuarine waters in Patagonian fjords. Sci. Total Environ. 798, 149241.
Peterson, B.J., Fry, B., 1987. Stable isotopes in ecosystem studies. Annu. Rev. Ecol. Syst. 18, 293–320.

Pickard, G.L., 1971. Some physical oceanographic features of inlets of Chile. J.Fish.Res.Board Can. 28, 1077–1106.
Pinilla, E., Castillo, M.I., Pérez-Santos, I., Venegas, O., Valle-Levinson, A., 2020. Water age variability in a Patagonian fjord. J.Mar.Syst. 210, 103376.
Pitcher, G.C., Louw, D.C., 2021. Harmful algal blooms of the Benguela eastern boundary upwelling system. Harmful Algae 102, 101898.
Pitcher, G.C., Figueiras, F.G., Hickey, B.M., Moita, M.T., 2010. The physical oceanography of upwelling systems and the development of harmful algal blooms. Prog. Oceanogr. 85, 5–32.
Pujol, C., Pérez-Santos, I., Barth, A., Alvera-Azcárate, A., 2022. Marine heatwaves offshore central and south Chile: understanding forcing mechanisms during the years 2016–2017. Front. Mar. Sci. 9, 800325.
Reche, P., Artal, O., Pinilla, E., Ruiz, C., Venegas, O., Arriagada, A., et al., 2021. CHONOS: oceanographic information website for Chilean Patagonia. Ocean Coast. Manag. 208, 105634.
Rodríguez-Villegas, C., Díaz, P.A., Salgado, P., Tomasetti, S.J., Díaz, M., Marín, S.L., et al., 2022a. The role of physico-chemical interactions in the sesonality of toxic dinoflagellate cyst assemblages: the case of NW Patagonian fjords system. Environ. Pollut. 311, 119901.
Rodríguez-Villegas, C., Figueroa, R.I., Pérez-Santos, I., Molinet, C., Saldías, G.S., Rosales, S.A., et al., 2022b. Continental shelf off northern Chilean Patagonia: a potential risk zone for the onset of Alexandrium catenella toxic bloom? Mar. Pollut. Bull. 184, 114103.
Roy, S., Montresor, M., Cembella, A., 2018. Key questions and recent research advances on harmful algal blooms in fjords and coastal embayments. In: Glibert, P.M., et al. (Eds.), Global Ecology and Oceanography of Harmful Algal Blooms, Ecological Studies. 232. Springer International Publishing AG, pp. 187–202 2018.
Salamena, G.G., Whinney, J.C., Heron, S.F., 2022. Vertical circulation due to deep-water renewal and phytoplankton blooms in the tropical fjord of Ambon Bay, eastern Indonesia. J.Mar.Syst. 234, 103776.
Sánchez, N., Gonzáles, H.E., Iriarte, J.L., 2011. Trophic interactions of pelagic crustaceans in Comau Fjord (Chile): their role in the food web structure. J. Plankton Res. 33 (8), 1212–1229.
Sandoval-Sanhueza, A., Aguilera-Belmonte, A., Basti, L., Figueroa, R.I., Molinet, C., Álvarez, G., et al., 2022. Interactive effects of temperature and salinity on the growth and cytotoxicity of the sh-killing microalgal species *Heterosigma akashiwo* and *Pseudochattonella verruculosa*. Mar. Pollut. Bull. 174, 113234.
Sauter, T., 2020. Revisiting extreme precipitation amounts over southern South America and implications for the Patagonian Icefields. Hydrol. Earth Syst. Sci. 24, 203–2016.
Schlitzer, R., 2015. Data analysis and visualization with Ocean Data View. CMOS Bull.SCMO 41, 9–13.
Selvaraj, K., Lee, T.Y., Yang, J.Y.T., Canuel, E.A., Huang, J.C., Dai, M., et al., 2015. Stable isotopic and biomarker evidence of terrigenous organic matter export to the deep sea during tropical storms. Mar. Geol. 364, 32–42.
Shikata, T., Nagasoe, S., Matsubara, Y., Yamasaki, Y., Shimasaki, Y., Oshima, Y., et al., 2007. Effects of temperature and light on cyst germination and germinated cell survival of the noxious raphidophyte *Heterosigma akashiwo*. Harmful Algae 6, 700–706.
Sibson, R., 1981. A Brief Description of Natural Neighbor Interpolation Interpreting Multivariate Data. John Wiley, Chichester.
Sievers, A.H., Silva, N., 2008. Water masses and circulation in austral Chilean channels and fjords. In: Silva, N., Palma, S. (Eds.), Progress in the Oceanographic Knowledge of Chilean Inner Waters, From Puerto Montt to Cape Horn. Comité Oceanográfico Nacional - Pontificia Universidad Católica de Valparaíso, Valparaíso, Chile, pp. 53–58.
Steinman, A.D., Lamberti, G.A., Leavitt, P.R., Uzarski, D.G., 2017. Biomass and Pigments of Benthic Algae Methods in Stream Ecology. 1, pp. 223–241.
Strickland, J.D., Parson, T., 1972. A practical hand book of seawater analysis. Fisheries Research Board of Canada. Bulletin, Second edition167.
Suárez-Isla, B.A., López-Rivera, A., Hernández, C., Clément, A., Guzmán, L., 2002. Impacto económico de las floraciones de microalgas nocivas en Chile y datos recientes sobre la ocurrencia de veneno amnésico de los mariscos. In: Sar, E., Ferrario, M.E., Reguera, B. (Eds.), Floraciones Algales Nocivas En El Cono Sur Americano. Instituto Español de Oceanografía, pp. 257–268.
Sutula, M., Kudela, R., Hagy III, J.D., Harding Jr., L.W., Senn, D., Cloern, J.E., et al., 2017. Novel analyses of long-term data provide a scientific basis for chlorophyll-a thresholds in San Francisco Bay. Estuar. Coast. Shelf Sci. 197, 107–118.
Townhill, B.L., Tinker, J., Jones, M., Pitois, S., Creach, V., Simpson, S.D., et al., 2018. Harmful algal blooms and climate change: exploring future distribution changes. ICES J. Mar. Sci. 75, 1882–1893.
Trainer, V.L., Pitcher, G.C., Reguera, B., Smayda, T.J., 2010. The distribution and impacts of harmful algal bloom species in eastern boundary upwelling systems. Prog. Oceanogr. 85, 33–52.
Twiner, J.M., Dixon, S.J., Trick, C.G., 2001. Toxic effects of *Heterosigma akashiwo* do not appear to be mediated by hydrogen peroxide. Limnol. Oceanogr. 46, 1400–1405.
Twiner, J.M., Dixon, S.J., Trick, C.G., 2004. Extracellular organics from specific cultures of *Heterosigma akashiwo* (Raphidophyceae) irreversibly alter respiratory activity in mammalian cells. Harmful Algae 3, 173–182.
Utermöhl, H., 1958. Zur Vervollkomnung der quantitativen phytoplankton-Methodik. Mitt. Int. Ver. Theor. Angew. Limnol. 9, 1–38.
Van Dolah, F.M., 2000. Marine algal toxins: origins, health effects, and their increased occurrence. Environ. Health Perspect. 108, 133–141.
Verado, D.J., Froelich, P.N., McIntyre, A., 1999. Determination of organic carbon and nitrogen in marine sediments using the Carlo Erba NA-1500 Analyzer. Deep Sea Res. I (37), 157–165.
Villalobos, V.I., Valdivia, N., Fösterra, G., Ballyram, S., Espinoza, J.P., Wadham, J.L., et al., 2021. Depth-dependent diversity patterns of rocky subtidal macrobenthic communities along a temperate fjord in Northern Chilean Patagonia. Front. Mar. Sci. 8, 635855.
Watts, L.J., 1994. The Roles of Hydrographic and Biogeochemical Processes in the Distribution of Dissolved Inorganic Nutrients in a Scottish Sea-loch System. University of Southampton, Southampton, The UK.
Watts, L., Rippeth, T., Edwards, A., 1998. The roles of hydrographic and biogeochemical processes in the distribution of dissolved inorganic nutrients in a Scottish sea-loch: consequences for the spring phytoplankton bloom. Estuar. Coast. Shelf Sci. 46, 39–50.
Wells, M.L., Trainer, V.L., Smayda, T.J., Karlson, B.S., Trick, C.G., Kudela, R.M., et al., 2015. Harmful algal blooms and climate change: learning from the past and present to forecast the future. Harmful Algae 49, 68–93.
You, Y., 2002. A global ocean climatological atlas of the Turner angle: implications for double-diffusion and water-mass structure. Deep Sea Res. I (49), 2075–2093.